

1 **Genetic and environmental influences on the evolution of virulence in the HIV-**
2 **associated opportunistic human fungal pathogen *Cryptococcus neoformans***

3 Yiwu Yu^{1,10¶}, Yuanyuan Wang^{2,6,7¶}, Linghua Li^{3¶}, Xiaoqing Chen^{2,7¶}, Xinhua Huang²,
4 Huaping Liang⁵, Tong Jiang^{2,7}, Guojian Liao⁸, Min Chen⁹, Liping Zhu¹⁰, Muyuan Li⁸,
5 Tao Zhou⁸, Qinyu Tang¹, Jingjun Zhao^{1,4*} and Changbin Chen^{2,6*}

6 ¹ Department of Dermatology, Tongji Hospital, Tongji University School of Medicine,
7 Shanghai 200065, China

8 ² The Center for Microbes, Development and Health, Key Laboratory of Molecular
9 Virology and Immunology, Institute Pasteur of Shanghai, Chinese Academy of Sciences,
10 Shanghai 200031, China

11 ³ Institute of Infectious Disease, Guangzhou No.8 People's Hospital, Guangzhou 510060,
12 Guangdong, China

13 ⁴ Gusu School, Nanjing Medical University, Suzhou Municipal Hospital, The Affiliated
14 Suzhou Hospital of Nanjing Medical University, Suzhou 215002, Jiangsu, China

15 ⁵ State Key Laboratory of Trauma, Burns and Combined Injury, Department of Wound
16 Infection and Drug, Army Medical Center (Daping Hospital), Army Medical University,
17 Chongqing 400042, China

18 ⁶ Nanjing Advanced Academy of Life and Health, Nanjing 211135, Jiangsu, China

19 ⁷ University of Chinese Academy of Sciences, Beijing 100049, China

20 ⁸ College of Pharmaceutical Sciences, Southwest University, Chongqing 400715, China

21 ⁹ Department of Dermatology, Shanghai Key Laboratory of Medical Mycology,
22 Changzheng Hospital, Second Military Medical University, Shanghai, China

23 ¹⁰ Department of Infectious Diseases, Huashan Hospital, Fudan University, Shanghai
24 200040, China

25 * Address correspondence to Jingjun Zhao, zhaojingjun2015@aliyun.com

26 Changbin Chen, cbchen@ips.ac.cn

27 ¶These authors have contributed equally to this work.

28 **Affiliations**

29 Yiwu Yu: 784888698@qq.com

30 Yuanyuan Wang: yywang@ips.ac.cn

31 Linghua Li: llheliza@126.com

32 Xiaoqin Chen: xqchen@ips.ac.cn

33 Xinhua Huang: xhhuang@ips.ac.cn

34 Huaping Liang: 13638356728@163.com

35 Tong Jiang: tjiang@ips.ac.cn

36 Guojian Liao: gjliao@swu.edu.cn

37 Min Chen: chenmin9611233@163.com

38 Liping Zhu: zhulp@fudan.edu.cn

39 Muyuan Li: 18434390502@163.com

40 Tao Zhou: 455810979@qq.com

41 Qinyu Tang: 623082932@qq.com

42 **Abstract**

43 The fungus *Cryptococcus neoformans* is considered the leading cause of death in
44 immunocompromised patients. Despite numerous investigations concerning its
45 molecular epidemiology, there are only a few studies addressing the impacts of varying
46 factors on genotype-phenotype correlations. It remains largely unknown whether
47 genetic and environmental variabilities among isolates from different sources may have
48 dramatic consequences on virulence. In this study, we analyzed 105 Chinese *C.*
49 *neoformans* isolates, including 54 from HIV-infected patients, 44 from HIV-uninfected
50 individuals and 7 from a natural environment, to investigate factors influencing the
51 outcome of *C. neoformans* infection. MLST analysis clearly identified sequence type
52 (ST) 5 as the prevalent sequence type in all clinical isolates and interestingly, genotypic
53 diversities were observed in isolates from both HIV-uninfected individual and natural
54 environment but not those from HIV-infected patients. Moreover, we found that
55 compared to those from HIV-infected patients, the isolates from HIV-uninfected
56 individuals exhibited enhanced virulence-associated traits including significantly
57 elevated capsule production and melanin formation, increases in survival in human
58 cerebrospinal fluid (CSF), less effective uptake by host phagocytes, and higher
59 mortality in a mouse model of cryptococcosis. Consistently, pathogenic phenotypes
60 were associated with CD4 counts of patients, implying environmental impact on within-
61 host *C. neoformans* virulence. Importantly, a large-scale whole-genome sequencing
62 analysis revealed that genomic variations within genes related to specific functions may
63 act as a vital driving force of host intrinsic virulence evolution. Taken together, our
64 results support a strong genotype-phenotype correlation suggesting that the pathogenic

65 evolution of *C. neoformans* could be heavily affected by both genetic and
66 environmental factors.

67 **Key words:** *Cryptococcus neoformans*; Virulence; Genotype-phenotype correlation;
68 Environmental factors; Genetic variants.

69 **Introduction**

70 Cryptococcosis refers to a major invasive fungal infection caused by the encapsulated
71 yeast species of the genus *Cryptococcus*, particularly *Cryptococcus neoformans* and
72 *Cryptococcus gattii*. *C. neoformans* contains two varietal forms, *C. neoformans var.*
73 *grubii* and *C. neoformans var. neoformans* [1, 2], and is distributed worldwide. In
74 comparison, *C. gattii* was originally thought to be restricted only in tropical and
75 subtropical districts but now this species was recognized in expanded temperate regions
76 due to an outbreak of cryptococcosis on Vancouver Island, Canada [3]. The prevalence
77 of cryptococcosis has increased in the past decade, and nearly a million cases of
78 cryptococcal meningitis are diagnosed annually around the world, mainly in
79 immunocompromised patients due to Human Immunodeficiency Virus (HIV) infection,
80 organ transplantation, cytotoxic chemotherapy, and corticosteroid use [4, 5]. Clinical
81 isolates of the *C. neoformans* and *C. gattii* species complexes are responsible globally
82 for 15 to 30% of deaths in HIV/AIDS patients due to cryptococcal meningitis [6].
83 Meanwhile, *C. neoformans* accounts for the most common cause of meningitis in HIV
84 adults in sub-Saharan Africa [6].

85 Phylogenetic analyses, as well as a number of genotyping studies, are being conducted
86 using clinical and environmental *C. neoformans* isolates collected all over the world, in
87 order to lay the basis for a comprehensive picture of the global genetic structure of this
88 fungus [7, 8], and significant genetic diversities are observed in the *C. neoformans*
89 species complex. All clinical *Cryptococcus* strains were initially treated as a single
90 species with a conserved name *C. neoformans* [9]. It was later classified into four
91 serotypes (A, B, C and D) based on Cryptococcal antigenic heterogeneity [10, 11].

92 Revised taxonomy further categorized the serotype B and C isolates to *C. gattii* [12],
93 while *C. neoformans* encompassed three major serotypes including *C. neoformans* var.
94 *grubii* (serotype A), *C. neoformans* var. *neoformans* (serotype D) and the hybrid
95 serotype AD [1]. Moreover, the *C. neoformans* species complex consists of two
96 evolutionary divergent species, *C. neoformans* and *C. deneoformans*, as well as their
97 associative hybrids (*C. neoformans* × *C. deneoformans*). Of the two lineages, *C.*
98 *neoformans* exhibited a worldwide distribution causing among 95% of cryptococcal
99 infections and >99% in AIDS individuals, whereas *C. deneoformans* is more frequent
100 in Europe and less virulent [13-15]. Due to a rapid development of molecular biology
101 techniques including PCR fingerprinting, amplified fragment length polymorphism
102 (AFLP) analysis, multilocus sequencing MLST and whole-genome sequencing [16-19],
103 the relatedness of isolates at a molecular level has revolutionized our ability to
104 differentiate among molecular types of the genus *Cryptococcus*. It is now well
105 appreciated that *C. neoformans* can be divided into at least five major molecular types
106 (AFLP1/VNI, AFLP1A/VNB/VNII, AFLP1B/VNII, AFLP3/VNIII and AFLP2/VNIV)
107 [2, 18, 20]. Among them, *C. neoformans* var. *grubii* (serotype A/VNI) was found to
108 naturally reside on avian excreta and trees, have a worldwide distribution, and
109 contribute to over 80% of cryptococcosis [21]. Similar to the VNI clade, the VNII clade
110 is also globally distributed. However, *C. neoformans* var. *grubii* (serotype A/VNB) was
111 primarily found in sub-Saharan Africa and South America [22, 23]. Moreover, *C.*
112 *neoformans* var. *neoformans* (serotype D/VNIV) was mostly found in Western Europe
113 and South America and the *C. neoformans* hybrid (serotype AD/VNIII) showed a
114 higher prevalence in the Mediterranean area of Europe [2, 24]. Collectively, these
115 observations strongly suggest that molecular types of the *C. neoformans* isolates not
116 only differ in their serological, epidemiological and ecological characteristics, but also

117 exhibit diverse features on clinical presentations, antifungal susceptibility and
118 therapeutic outcomes [16, 25, 26].

119 Recently, a growing body of evidence highlights the impact of *C. neoformans* genotype
120 on the host disease outcome. For example, an epidemiological study by Wiesner *et al.*
121 found that genotypes of *C. neoformans* isolates from HIV/AIDS patients in Uganda
122 could be grouped into three distinct clonal clusters within the VNI clade and among
123 them, both ST93 and ST77 isolates showed the highest mortality risk [27].
124 Comparatively, a similar study using clinical isolates from South African HIV/AIDS
125 patients identified that ST32 isolates in the VNB clade exhibit worse patient outcome
126 [28] and moreover, genotypic analysis of clinical *C. neoformans* isolates from Brazil
127 revealed that ST93 in VNI clade is the most prevalent sequence type in HIV-infected
128 patients [23]. However, a strikingly different link between isolate genotype and disease
129 outcome was found in Asian countries, where *C. neoformans* infections are often
130 observed in immunocompetent individuals [29] and ST5 represents the major sequence
131 type in *C. neoformans* isolates from East Asian countries including China, Japan,
132 Vietnam and South Korea [30, 31]. For example, a study using 136 Vietnamese clinical
133 isolates of *C. neoformans var. grubii* revealed that ST5 isolates are responsible for 82%
134 of infections in HIV uninfected patients, compared to only 35% cases in HIV infected
135 patients [31]. In addition, MLST analysis of Chinese clinical *C. neoformans* isolates by
136 different research groups also identified ST5 as the predominant sequence type [32].
137 Of course, notable exceptions exist. For instance, studies have indicated that ST4 and
138 ST6 are the major MLST types in *C. neoformans var. grubii* isolates of Thailand
139 whereas ST93 turns to be the dominant isolates from India and Indonesia [30, 33].
140 Interestingly, detailed information regarding genetic diversity of the isolates suggests

141 that those from Thailand posit an evolutionary origin in African and the strains from
142 China may have the same African origin but were expanded more flexibly and globally
143 [5, 33]. Taken together, these studies highlight the presence of global genetic diversities
144 in *C. neoformans* isolates and argue the correlation between pathogen genotype and
145 patient phenotype. Of course, it is important to note that the patho-phenotypic variations
146 of *C. neoformans* isolates cannot be fully explained by genotypic diversity, and other
147 factors should also be considered.

148 Factors determining disease prevalence and species specificity are relatively unknown,
149 but are speculated to be associated with the host immune response, genetic varieties,
150 and virulence factors. For example, the type 1 helper T-cell (Th₁) response could
151 stimulate classical activation of macrophages and eliminate internalized cryptococcal
152 cells, however, the type 2 helper T-cell (Th₂) response was found to promote the
153 disseminated, uncontrolled cryptococcal infection [34, 35], suggesting that patients
154 exhibiting different immune responses to cryptococcal infections could yield varied
155 clinical outcomes. Moreover, the distribution and prevalence of the molecular types
156 appear to be highly relevant to geographical locations, the size of samples and host
157 characteristics [1, 2]. For example, previous studies suggested that *C. neoformans*
158 serotype A is one of the most common varieties and account for the majority of
159 cryptococcal infections in Asia, especially in HIV-AIDS patients [34, 35]. In addition,
160 studies showed that a list of virulence factors including the presence and size of the
161 polysaccharide capsule, melanin production by laccase, cell size variation, growth at
162 37 °C and secretion of enzymes such as phospholipase, proteinase and urease,
163 sphingolipid utilization, contribute to *C. neoformans* pathogenicity [36, 37]. However,

164 it remains unclear whether these factors were correlated, and if so, how to affect the
165 evolution of *C. neoformans* pathogenicity?

166 In an attempt to interpret the molecular epidemiology of *Cryptococcus* species, the
167 strain differences in genotype and phenotype, as well as the impacts of genetic and
168 environmental correlations on the evolution of fungal virulence, we analyzed a
169 collection of 105 clinical and environmental isolates of *C. neoformans* in China,
170 including those isolated from HIV-infected patients and HIV-uninfected individuals.
171 The genotype of each isolate was determined by MLST and the evaluation of
172 pathogenic phenotypes was performed *in vitro* and *in vivo*. Moreover, the genotype-
173 phenotype correlations were further assessed by genetic variations through the genome-
174 wide linkage and association analyses. Our results compare the impacts of genetic and
175 environmental factors on affecting the correlation between genotype and phenotype of
176 *C. neoformans* isolates, and provide *in vitro* and *in vivo* data to support the influence of
177 genetic and environmental changes on genotypic and pathogenic variations.

178 **Materials and methods**

179 **Ethics statement**

180 All of animal experiments were performed in compliance with the Regulations for the
181 Care and Use of Laboratory Animals issued by the Ministry of Science and Technology
182 of the People's Republic of China, which enforces the ethical use of animals. The
183 protocol was approved by IACUC at the Institut Pasteur of Shanghai, Chinese Academy
184 of Sciences (Permit Number: 160651A).

185 **Strains**

186 A total of 105 isolates of *C. neoformans* strains were assayed in this work, including
187 44 from the HIV-uninfected patients (HIV-u group), 54 from the HIV-infected patients
188 (HIV-i group) and 7 from the nature (Env group). Clinical and laboratory records of all
189 patients were obtained from Guangzhou No.8 People's Hospital, Huashan Hospital,
190 Changzheng Hospital and Southwest University. The data collected for analysis
191 included age, gender, initial symptoms, HIV infection status and CD4⁺ T cell count (at
192 the time of diagnosis). The detailed information about each of the samples is presented
193 in **S1 Table**. Among these, 98 strains were isolated from cerebrospinal fluid (CSF)
194 samples (n = 90) and blood cultures (n = 8). *C. neoformans* clinical isolates were single
195 colony purified on YPD medium and then maintained as glycerol stocks at -70°C for
196 long-term storage. A detailed information about each sample is listed in **S2 Table**. Each
197 strain was streaked and grown as a single colony on yeast peptone dextrose (YPD)
198 medium prior to use.

199 A list of reference strains was included in this study, including international strains used
200 for phylogenetic analysis (H99 in USA, WM148 and WM626 in Australia, ST93 in
201 Brazil) and standard strains for *in vitro* and *in vivo* assays (JEC20 and H99). All strains
202 were maintained on yeast peptone dextrose (YPD) medium prior to use.

203 **DNA extraction**

204 Isolates were grown on Sabouraud dextrose agar slants for 48 h. Single colonies were
205 isolated, re-inoculated in 10ml of liquid medium, and grown at 30°C for 24 h. The cells
206 were collected by centrifugation and genomic DNA was extracted using the
207 cetyltrimethylammonium bromide (CTAB) DNA isolation method as previously
208 described [38].

209 **Multilocus Sequence Typing (MLST)**

210 Multilocus sequence type analysis was carried out using the seven ISHAM consensus
211 loci (*CAP59*, *GPDI*, *IGSI*, *LACI*, *PLBI*, *SODI*, *URA5*), following a standard
212 procedure [18, 22]. All primers used in this study were described previously [27] and
213 listed in **S6 Table** .

214 **Phylogenetic analysis**

215 The sequences were aligned with the computer program CLUSTAL W and a
216 phylogenetic tree was drawn based on the neighbor-joining (NJ) model. The
217 evolutionary distances were computed based on the *p*-distance, and all gaps were
218 eliminated. A bootstrap analysis was performed with 1,000 replicates [39].

219 **Assays for melanization and capsule formation**

220 Melanin production was measured by comparing pigmentation of strains grown on L-
221 DOPA media to reference strains with strong (H99) and weak (JEC20) melanization,
222 using a method described previously [40]. Relative melanization scores of zero (equal
223 to JEC20), one to four (between JEC20 and H99) and five (more than or equal to H99)
224 were assigned to the strains based on comparison with the reference strains grown on
225 the same plate.

226 The capsule induction assay was performed using a method described previously [41],
227 with some modifications. In brief, stationary-phase fungal cultures were washed and
228 resuspended in PBS. Cells were diluted 1/100 in capsule induction medium [10%
229 Sabouraud dextrose medium in 50mM MOPS buffer (pH 7.3)] and incubated at 30 °C
230 and 180rpm for 48h. The size of capsule was measured by staining the cells with India
231 ink and imaging at a magnification of $\times 63$ under a light microscope. As described by

232 Fernandes *et al.* [42], the diameters of the whole cell (yeast cell + capsule) and the cell
233 body (the cell wall only) were each measured using Image J software, and the mean of
234 the values was calculated for 10-20 cells for each isolate.

235 The identification of mating types was carried out in a classical PCR analysis using the
236 mating type and serotype specific primers [43]. All primers are listed in **S6 Table**.

237 **Infection of macrophages with *Cryptococcus***

238 Phagocytosis assays were performed with the murine macrophage-like cell line J774,
239 using a method previously described [44, 45]. Briefly, macrophage cells in DMEM
240 supplemented with 10% heat-inactivated fetal bovine serum (FBS), 1 mM L-glutamine,
241 and 1% penicillin-streptomycin (Sigma-Aldrich) were plated into each well of a 24-
242 well tissue culture plate for 24 hours at 37°C with 5% CO₂. Macrophage cells ($1.5 \times$
243 10^5) were incubated in serum-free DMEM medium for 2 hours, activated with 15µg/ml
244 phorbol myristate acetate (PMA) (Sigma-Aldrich) for 30-60 minutes, and then co-
245 incubated with *C. neoformans* yeast cells opsonized by a monoclonal antibody
246 (C66441M, purchased from Meridian Life Science, Inc) for 2 hours at 37°C with 5%
247 CO₂ (MOI=1:10). Extracellular yeast cells were removed by extensive washes with
248 prewarmed PBS. The extent of *Cryptococcus* phagocytosis was calculated as the
249 number of cryptococci internalized by macrophages 2 hours after infection. Results
250 were expressed as the mean of 3 to 4 experimental repeats.

251 **CSF survival assay**

252 Human cerebrospinal fluid (CSF) was pooled from Shanghai Changzheng Hospital
253 patients receiving serial therapeutic lumbar punctures, collected anonymously from
254 populations of at least 15 patients. The human CSF was fully examined for parameters,

255 including white cell count, protein and glucose levels, within the normal ranges and for
256 the absence of antifungal drugs. Clinical isolates of *C. neoformans* were replicated in
257 48-well plates in Sabouraud dextrose broth (SDB) and incubated at 37°C for 3-4 days
258 until saturation. Cultures were then diluted, inoculated into CSF at a concentration of
259 $1\sim 2 \times 10^6$ cells/ml, and incubated at 37°C for 96 hours. As described previously [45],
260 aliquots were collected at different time points (0,12, 24, 36,72 and 96 hours after
261 inoculation) and plated on Sabouraud dextrose agar (SDA) media for CFU counts. The
262 survival slope was determined as the mean rate of increase or decrease in cryptococcal
263 counts after CSF treatment, by averaging the slope of the linear regression of \log_{10}
264 CFU/ml over time for each strain.

265 **Virulence studies**

266 A well characterized murine inhalation model of cryptococcosis was used [46] . Briefly,
267 three isolates were randomly picked from each of the three groups and individually
268 grown overnight in liquid YPD cultures at 30 °C . All strains tested are ST5, except for
269 one environmental strain (Env #103; ST39). Cells were counted using a hemocytometer
270 and the yeast suspension with a final concentration of 1×10^7 cells/ml was prepared.
271 6-8 week-old female C57BL/6 mice were anesthetized by intraperitoneal injection of
272 ketamine (75 mg/kg) and medetomidine (0.5-1.0 mg/kg) and a 50 μ L volume of the
273 yeast suspension (1×10^5 cells) was intranasally injected. 8 mice were infected per
274 inoculum. Mice were monitored several times a week until the observance of disease
275 symptoms (weight loss, ruffled fur, shallow breathing, abnormal gait and lethargy) and
276 then monitored daily. Mice were sacrificed by CO₂ inhalation followed by cervical
277 dislocation when signs of severe morbidity, including significant weight loss, abnormal
278 gait, hunched posture and swelling of the cranium, were clearly displayed. A Kaplan-

279 Meier method was employed to analyze survival curves using GraphPad Prism 6.0
280 software. Differences in the median survival among species were determined by
281 performing the log-rank test [38, 47].

282 **Whole Genome Sequencing**

283 28 *C. neoformans* strains isolated from HIV-infected patients and HIV-uninfected
284 patients were subjected to whole-genome sequencing. In order to minimize the
285 genotype impact on the sequencing, all 28 strain were selected ST5. Next generation
286 sequencing library preparations were constructed following the manufacturer's
287 protocol (NEBNext[®] Ultra[™] DNA Library Prep Kit for Illumina[®]). For each sample,
288 1 µg genomic DNA was randomly fragmented to <500 bp by sonication (Covaris S220)
289 and DNA fragments were treated with End Prep Enzyme Mix for end repairing, 5'
290 Phosphorylation and dA-tailing in one reaction, followed by a T-A ligation to add
291 adaptors to both ends. Size selection of Adaptor-ligated DNA was then performed using
292 AxyPrep Mag PCR Clean-up (Axygen) and fragments of ~410 bp (with the
293 approximate insert size of 350 bp) were recovered. Each sample was then amplified by
294 PCR for 8 cycles using P5 and P7 primers, with both primers carrying sequences which
295 can anneal with flowcell to perform bridge PCR and P7 primer carrying a six-base index
296 allowing for multiplexing. The PCR products were cleaned up using AxyPrep Mag
297 PCR Clean-up (Axygen), validated using an Agilent 2100 Bioanalyzer (Agilent
298 Technologies, PaloAlto, CA, USA), and quantified by Qubit2.0 Fluorometer
299 (Invitrogen, Carlsbad, CA, USA). The whole genome of each strain was sequenced
300 using Illumina NovaSeq6000 PE150 at the Beijing Novogene Bioinformatics
301 Technology Co., Ltd.

302 **Data analysis**

303 The raw data was removed the sequences of adaptors, polymerase chain reaction (PCR)
304 primers, content of N bases more than 10% and bases of quality lower than 20 by using
305 Cutadapt (V1.9.1). Then the clean data was mapped to the *C. neoformans* H99 reference
306 genome FungiDB (<http://fungidb.org/fungidb/>) by using BWA (V0.7.17) and mapping
307 results were processed by Picard (V1.119) to remove duplication. SNPs/InDels were
308 called by the GATK Unified Genotyper (V3.8.1) and Annotated by Annovar (V21 Apr
309 2018). GO-term analysis of processes enriched among specific gene sets of HIV-i and
310 HIV-u group was performed using the topGO (V2.34.0).

311 **Statistics**

312 Data were presented as mean \pm standard error of the mean (SEM). Statistical analysis
313 was performed by one-way analysis of variance (ANOVA) in GraphPad Prism 6.0
314 software (San Diego, CA). The following *p*-values were considered: * $p < 0.05$; ** p
315 < 0.01 ; *** $p < 0.001$; **** $p < 0.0001$.

316 **Data availability**

317 The authors declare that the data supporting the findings of this study are available
318 within the article and its supplementary information files, or are available upon request
319 to the corresponding authors. Whole-genome sequences are available at NCBI under
320 BioProject ID: PRJNA680424.

321 **Results**

322 **Characterization of clinical presentation and outcome**

323 In order to study the correlations amongst environmental conditions, immune
324 inflammatory syndrome and other clinical outcomes, we collected a total of 98
325 clinical isolates of *C. neoformans* that were recovered from cerebrospinal fluid (CSF)
326 samples (n=90) and blood cultures (n=8) of 98 patients hospitalized at different
327 locations of China. Among them, 54 strains are from HIV-infected patients and 44 are
328 from HIV-uninfected individuals. Clinical laboratory data was investigated from 95
329 patients (three patients' data was somehow missed). Both **Table 1** and **S1 Table**
330 showed the detailed information about the influence of common symptoms on clinical
331 outcome that could be used to Fig out the relationships between isolate origin and
332 clinical consequences. The majority of patients were male (74; 77.9%), the age ranged
333 from 21 to 68 years and the mean age was 41 ± 11 years.

334 Among them, the most common presenting symptom was headache (70%), especially
335 in HIV-infected patients (73%). Comparatively, the HIV-uninfected patients were less
336 frequently found to have high fever but they had more severe symptoms such as seizure,
337 cerebral herniation and cerebellar signs. Moreover, 39 out of 51 HIV-infected patients
338 presented CD4⁺ T-cell counts below 50 /mm³. However, the mean \pm SD of CD4⁺ T-
339 cell counts from 44 HIV-uninfected individuals was 381 ± 92 mm³/ml. These results
340 are consistent with a recent study that the HIV-associated cryptococcal meningitis
341 normally occurs in patients with higher CD4 counts [48].

342 **MLST and phylogenetic analyses**

343 The 98 clinical isolates, together with 7 environmental strains collected from pigeon
344 excreta, were classified into three groups (HIV-u group: 44 strains from HIV-
345 uninfected individuals; HIV-i group: 54 strains from HIV-infected patients; Env group:

346 7 environmental strains from the pigeon excreta). After colony purification, all 105
347 isolates were analyzed to determine their genotypes by Multilocus Sequence Typing
348 (MLST), based on a formal study that described a consensus sequence-based
349 epidemiological typing scheme, using seven housekeeping genes (*CAP59*, *GPD1*, *IGS1*,
350 *PLB1*, *LAC1*, *SOD1*, *URA5*) [18]. For each strain, locus allele identifiers were used and
351 combined to generate a sequence type (ST) representing the strain genotype [49].
352 MLST analysis of all 105 isolates demonstrated the presence of 9 sequence types (ST),
353 including ST5 (n = 94; 89.5%), ST359 (n = 2; 1.9%), ST2 (n = 2; 1.9%), and ST39 (n
354 = 2; 1.9%), ST360 (n=1; 0.9%), ST194 (n=1; 0.9%), ST31 (n=1; 0.9%), ST93 (n=1;
355 0.9%), ST195 (n=1; 0.9%) (**Fig 1A**). To our surprise, we found in **S2 Table** that all
356 isolates from HIV-i group were restricted to a single ST (ST5). In comparison, STs
357 identified in isolates from HIV-u and Env groups were more diverse, as we observed
358 that strains from HIV-u group contain 8 STs, including ST5 (n=36), ST359 (n=2), ST2
359 (n=1), ST360 (n=1), ST194 (n=1), ST31 (n=1), ST93 (n=1) and ST195 (n=1), and
360 strains from the Env group also harbor 3 STs, including ST5 (n=4), ST39 (n=2) and
361 ST2 (n=1).

362 In addition, a phylogenetic analysis was performed among strains from different
363 geographic locations (China, Australia, Brazil and USA), based on the concatenated
364 sequences of MLST loci (**Fig 1B**). The phylogenetic tree revealed that ST5 was quite
365 close to ST359 and ST360, while ST39 was far from other identified STs. Moreover,
366 we concluded from this study that the major epidemic clone of *C. neoformans var.*
367 *grubii* in China was ST5 regardless of their origins. Actually, similar patterns were
368 observed in previous studies using strains isolated from HIV-uninfected individuals of
369 China [7, 50].

370 As shown in **Fig 1A**, we found that the majority of the isolates in this collection were
371 of one sequence type (ST5), which was 54 out of 54 in the HIV-i group, 36 out of 44
372 in the HIV-u group and 4 out of 7 in the Env group, prompting us to evaluate the
373 potential relevance of the isolates to virulence according to their origins other than the
374 STs.

375 ***In vitro* and *ex vivo* phenotyping**

376 *C. neoformans* produces several important virulence factors, most notably the mating
377 type, polysaccharide capsule, and melanin production. Studies have shown that mating
378 type can influence virulence through cell type (*MAT α* or *MATa*) and the function of
379 specific genes such as those related to MAP kinase pathway [51-53]. The mating types
380 and serotypes of all isolates were determined by multiplex PCR using specific primers
381 described previously [18]. Among the 105 strains evaluated, 104 were characterized as
382 serotype A *MAT α* (*A α*) and only one strain was found to be serotype A *MATa* (*Aa*)
383 (**S1 Fig**).

384 Melanin is another major virulence factors in *C. neoformans*. We carried out *in vitro*
385 assays to evaluate the ability of all 105 isolates to produce melanin by patching on
386 medium containing L-DOPA (L-3,4-dihydroxyphenylalanine) [54]. A scoring method,
387 based on K-means clustering analysis, was employed to evaluate melanin production
388 of all tested isolates. Two reference strains (JEC20 and H99) were used as experimental
389 controls, given the fact that the strain JEC20 has been reported to produce almost no
390 melanin whereas the clinical isolate H99 exhibits strong melanization [55]. As shown
391 in **Fig 2 and S2 Fig**, we found that strains in HIV-u group produce significantly higher
392 levels of melanin, as showed by dark pigments, when compared to those in HIV-i group

393 ($p < 0.0005$ by Tukey adjusted t-test), implying that the clinical isolates from the two
394 groups may have differences in pathogenicity.

395 This notion was further supported by assaying the polysaccharide capsule formation of
396 each isolate. Capsule induction of each isolate was achieved under nutrient-limiting
397 conditions (capsule induction medium; 10% Sabouraud dextrose medium in MOPS
398 buffered at pH 7.3) and measured by staining with India ink, following a protocol
399 described in Materials and Methods. The capsule size of each strain was determined by
400 Adobe Photoshop software (Adobe Inc, USA) and the data was further analyzed by a
401 K-means clustering algorithm. We observed that after induction, strains in HIV-u group
402 generate much larger capsules than those in HIV-i group, although their sizes are almost
403 indistinguishable under un-induced condition (**Fig 2 and S3 Fig**).

404 The ability of *C. neoformans* to survive in the cerebrospinal fluid (CSF) has been
405 found to contribute to the cryptococcal virulence due to its presence in clinical
406 specimens and production of life-threatening disease in the central nervous system
407 (CNS). To further evaluate the pathogenic variabilities between cryptococcal strains
408 from HIV-infected and uninfected individuals, we assayed the survival of all 98
409 clinical isolates in human CSF. When compared to those from the HIV-I group,
410 isolates from the HIV-u group exhibited more resistant to killing by human CSF (**Fig**
411 **3A**). Moreover, we found a positive correlation between CSF survival and capsule
412 size ($r = 0.6737$, $p < 0.0001$; **Fig 3B**). These data sustain the proposition that strains in
413 HIV-u group appear to be more virulent than host in HIV-I group.

414 In addition, many studies have emphasized the role of fungal internalization by
415 macrophages as a critical virulence factor in cryptococcal disease [56, 57].

416 Interestingly, when the macrophage uptake of *C. neoformans* cells was evaluated in
417 the established murine macrophage-like cell line J774, we observed that isolates from
418 the HIV-i group were phagocytosed at a higher rate than those from the HIV-u group
419 (**Fig 3C**), and this trait could be explained by differences in capsule size, since
420 phagocytic uptake and capsule size is inversely correlated in this set of isolates ($r = -$
421 0.5345 , $p < 0.0001$; **Fig 3D**). Actually, our results are consistent with previous reports
422 that the capsule passively inhibits phagocytosis of *C. neoformans* by macrophages
423 and the capsule-dependent anti-phagocytic activity represents a major virulence
424 attribute [45, 58, 59].

425 Taken together, both *in vitro* and *ex vivo* phenotypic assays suggest that compared to
426 those from the HIV-infected patients, the clinical isolates derived from the HIV-
427 uninfected individuals exhibit significantly enhanced capsule production and melanin
428 formation, higher increases in survival in CSF, and less effective uptake by host
429 phagocytes, which represent key factors associated with *Cryptococcus* pathogenicity
430 [60, 61].

431 ***In vivo* virulence analyses**

432 Given the observed differences in capsule and melanin production between strains from
433 HIV-uninfected and infected groups, we sought to ask whether strain origins may affect
434 *C. neoformans* virulence. We conducted an *in vivo* virulence analysis using a mouse
435 model of cryptococcosis [46]. Groups of 6-8-week female C57BL/6 mice (8 mice per
436 group) were inoculated intranasally with strains from the three groups (we randomly
437 picked three strains in each group), as well as the H99 strain serving as a control. All
438 isolates tested are ST5, except for one environmental strain (Env #103; ST39). Mice

439 were sacrificed by CO₂ inhalation followed by cervical dislocation when signs of severe
440 morbidity, including weight loss, abnormal gait, hunched posture and swelling of the
441 cranium, were clearly observed. Consistent with a previous study [46], the control strain
442 H99 caused a lethal infection by day 20. As expected, we observed that mice inoculated
443 with the strains of HIV-u group showed similar or even worse signs of disease as the
444 control strain. In contrast, mice inoculated with strains from both HIV-i and Env groups
445 showed almost identical survival rates (**Fig 3E**), and the strains in these two groups are
446 much less virulent than those in HIV-u group.

447 Thus, consistent with the results obtained from *in vitro* and *ex vivo* assays, our *in vivo*
448 analysis also indicated that clinical isolates of *C. neoformans* from different hosts
449 exhibit differentiation of virulence phenotypes, implying the importance of
450 environmental factors on the evolution of virulence.

451 **Genetic variations**

452 Studies have shown that microbial pathogens evolve a broad range of intrinsic and
453 extrinsic strategies to acquire and modulate existing virulence traits in order to achieve
454 successful colonization in the host [62]. In addition to the impact of environmental
455 factors, pathogenicity of *C. neoformans* must be also influenced at the genetic level,
456 since genetic variation in the genome is recognized as a fact of life in microbes,
457 allowing pathogens to adapt to their chosen host and also to resist clearance by the host.
458 Moreover, whole genome-resequencing technology has been used as a powerful tool to
459 explore the genetic mechanism in fungi and fungal-host interaction [63]. Hence, we
460 sequenced and assembled the whole genomes of 28 strains in the collection (ST5), 14
461 from HIV-u group and 14 from HIV-i group (the strains were chosen based on the

462 patients' parameters, including close age, sex and several other factors within the same
463 group), and performed a comparative study to identify potential correlations between
464 genetic variation and virulence, by comparing the genome difference of 28 isolates
465 against the finished reference strain H99. Quality control analyses of our sequencing
466 data were summarized in **S3 Table**. Overall, sequencing the 28 isolates yielded a total
467 of 65 Gb containing 436 million raw reads, with an average of 15.6 million reads for
468 each sample. The raw reads were further filtered by removing the low quality reads and
469 duplicate reads, producing 52 Gb containing 349 million high quality reads.
470 Approximate 94.8% of the clean reads could be mapped to the H99 reference genome,
471 varied from 30.77 to 99.08% among different strains (**S4 Table**). These mapped
472 sequences were used for further analyses.

473 **S5 Table** lists the number of mutations observed in the 28 clinical isolates comparing
474 with the reference genome of H99. We identified a total of 65,106 variants, including
475 57,401 SNPs (single nucleotide polymorphism; 13,133 (22.9%) synonymous and
476 10,755 (18.7%) nonsynonymous) and 7,705 indels (insertions/deletions; 4,149 (53.8%)
477 InDel-Ins and 3,556 (46.2%) InDel-Del), across the genomes of 14 HIV-u isolates. In
478 comparison, our analysis across the genomes of 14 HIV-i isolates generated a total of
479 64,138 variants, with 56,655 SNPs (13,064 (23.1%) synonymous and 10,683 (18.9%)
480 nonsynonymous) and 7,483 indels (4,058 (54.2%) InDel-Ins and 3,425 (45.8%) InDel-
481 Del). The relationship between number of variants and gene was identified in **Fig 4A**
482 and the inset panel was magnified to show genes with at least 20 variants for
483 visualization purposes. The results showed that there was no significant difference in
484 both groups. As shown in **Fig 4B**, the majority of genes in both groups harbor relatively
485 few variants and there is no correlation between gene length and the number of variants,

486 indicating that the relative frequencies of genetic variations in these clinical isolates are
487 quite similar and appear to be independent of strain origins. In addition, we surprisingly
488 found in **Fig 4C** that the genes harboring more than 80 variants were almost identical
489 in all sequenced isolates of both groups, suggesting that differential virulence may not
490 be generalized to regions encompassing extreme genomic instability, instead, may be
491 attributed to genomic mutations of genes associated with specific functions.

492 Indeed, extensive analysis about the genome comparison between H99 and the clinical
493 isolates identified polymorphisms in these two groups. **Fig 5A** showed variants that
494 were common or specific in the isolates from HIV-u and HIV-i groups. We identified
495 55,292 common SNPs (we defined common variants as the ones that are found in more
496 than 7 isolates) in both groups, and only 628 and 648 variants specific for HIV-u and
497 HIV-i groups, respectively. Moreover, we found that compared to those specific SNPs
498 of HIV-i group, the isolates of HIV-u group exhibited a significant higher level of
499 variant enrichment at the intergenic region (54.05% vs 41.90%) but much less
500 abundance in both upstream and exonic regions (4.98% vs 9.49% and 19.16% vs
501 28.18%, respectively). Other locations, such as intronic, downstream and
502 ncRNA_exonic regions, showed no difference in variant distribution between the two
503 groups (**Fig 5B**). Furthermore, the 648 unique variants of isolates in HIV-u group were
504 associated with 329 genes whereas the 628 unique variants in HIV-i group counts for
505 206 genes.

506 Importantly, when we determined the functional categories of the unique genes
507 identified in each of the two groups using Gene Ontology (GO) Database, surprising
508 findings were obtained. Overall, the functions of the specific genes of each group could
509 be classified into three general directions (**Fig 6A, B and C**). In the biological process

510 category, the top highly enriched GO terms in HIV-i group include protein
511 glycosylation activity while those in HIV-u group were enriched in signal transduction
512 activity. In the cellular component, the GO terms of RISC complex and riboflavin
513 synthase complex were significantly enriched in HIV-i and HIV-u groups, respectively.
514 As for the molecular function category, genes with specific variations in strains of HIV-
515 i group showed a high percentage of metal/zinc ion binding process whereas those in
516 HIV-u group dominated in the process of oxidoreductase activity. Although isolates
517 from both HIV-i and HIV-u groups exhibit a large number of overlapping variants in
518 the genomes, there is a subset of genes in each group that harbor unique mutations and
519 account for different functions. The related functions and names of major mutated
520 genes differed in two groups were listed in **Table 2**. We observed that the functions of
521 HIV-i strain specific genes are mainly linked to microbial metabolism while those in
522 HIV-u group impinge their roles in stress response, signal transduction and drug
523 resistance. For example, the isolates from the HIV-u group harbored specific genetic
524 variants in the genes *SSK1*, *TCO2* and *PBS2* who have been found to be key players in
525 the fungal two-component system and the HOG signaling pathway and reported to
526 regulate stress responses, drug sensitivity, sexual development, differentiation and
527 virulence of *C. neoformans* [64, 65]. Moreover, specific mutations were also identified
528 in the genes like *RHO104/RIM20* and *APT4* in the isolates from HIV-uninfected
529 individuals but not in those from HIV-infected patients. Rho104/Rim20 are effectors
530 of the PKA signaling pathway and required for many virulence-associated phenotypes
531 such as titan cell formation in *C. neoformans* [66], and Apt4 is the P4-ATPase subunit
532 of the Cdc50 family and regulates iron acquisition and virulence in *C. neoformans* [67].
533 In comparison, most genes harboring specific mutations in the isolates of HIV-i group
534 are involved in metabolic processes, such as the MAPK signaling pathway (*SSK2*),

535 tryptophan biosynthesis (*TRP1*), riboflavin biosynthesis (*RIB3*), cell wall protein
536 glycosylation (*KTR3*) and cellular metabolism and compound biosynthesis (*KIC*, *HRK1*,
537 *KIN1*, *GPA3*, *FZC45*, *SNF102*, *URE7*, *DST1* and *BCK1*).

538 These data strongly suggest that compared to those isolated from HIV-infected patients,
539 *C. neoformans* strains from HIV-uninfected individuals need to evolve genetic
540 variations in a list of specific genes related to environmental adaptation, since microbes
541 have to confront with more rigor host environment, such as immune clearance.

542 **Discussion**

543 Cryptococcosis, primarily caused by *Cryptococcus neoformans* and *Cryptococcus*
544 *gattii*, is a primary opportunistic fungal infection that has been found to be associated
545 with patients with HIV infection. Of course, this fungal infection also occurs in other
546 underlying disorders, including immunosuppressant usage, transplantation, cancers and
547 diabetes mellitus *etc.* So far, studies on cryptococcosis in China have been carried out
548 mainly in HIV-uninfected patients [29]. In this study, we used a large number of *C.*
549 *neoformans* strains isolated from different sources, including those from the HIV-
550 infected and HIV-uninfected patients, as well as natural environment, and
551 systematically evaluated impacts of genetic and environmental factors on genotypes
552 and virulence-related phenotypes of these isolates. We observed strong correlations and
553 trends among the three different environments, which suggest that host environments
554 appear to play important roles in affecting the virulence of *C. neoformans* isolates.
555 Overall, strains isolated from the HIV-infected patients showed much lower virulence
556 when compared to those from the HIV-uninfected individuals and a natural
557 environment, indicating that *C. neoformans* pathogenicity has a great plasticity during

558 interaction with different hosts. Interestingly, the information from whole-genome
559 sequencing suggests that the high incidence of hotspot mutations may not be the major
560 factor that accounts for the differential virulence among the isolates derived from either
561 the HIV-i or HIV-u group. Instead, genomic variations within genes related to specific
562 functions may act as a major driving force of host intrinsic virulence evolution.

563 Broad epidemiology and molecular typing studies of *C. neoformans* and *C. gattii*
564 species complex have been reported all over the world, showing that genotypes are
565 distinctly related to geographical locations [2]. Originally we planned to study the
566 genotype-phenotype correlation using strains harboring different sequence types (ST).
567 Unexpectedly, our results identified that all of the 105 isolates belong to the molecular
568 type AFLP1/VNI and ST5 was the most common sequence type (n = 94; 89.5%),
569 although other STs were also identified using MLST, making it impossible to evaluate
570 the difference in the production of virulence factors between isolates from different STs.
571 Consistently, the observation that ST5 was the predominant sequence type that caused
572 human cryptococcosis in China was found to be the same case in most other Asian
573 countries [68]. A distinct genotypic characteristic of Chinese *C. neoformans* isolates
574 was apparent that ST5 represents the most prevalent genotype in clinical isolates from
575 both HIV-infected and -uninfected samples and comparatively, the genotypes of those
576 natural isolates (from pigeon droppings) are much more diverse. Furthermore, the data
577 currently available imply that the genotypic diversity in isolates from HIV-infected
578 patients appear to be more limited than those from HIV-uninfected individuals, and of
579 course, supporting this notion requires larger isolate collections and decent work in data
580 analyses.

581 Although strains with different genotypes harbor almost the same mating type, we
582 observed differences of these strains in melanin production and capsule formation.
583 Apparently, strains isolated from the HIV-uninfected patients produced significantly
584 more melanin than those isolated from the HIV-infected patients and the nature,
585 suggesting that once infected, a higher melanin biosynthesis of cryptococcal strains
586 might be triggered in response to a relatively stronger immune system, given that host
587 immune system has completely been dampened in HIV-infected patients. Considering
588 the prevalence of L-DOPA in the central nervous system [27], our results also proposed
589 that an increased melanin production in strains isolated from the HIV-uninfected
590 patients could potentially occur *in vivo* and promotes virulence, leading to an increase
591 in the mortality. Moreover, capsule generation in different strains yields similar results.
592 A previous study showed that capsule size in cryptococcal cells was found to differ
593 significantly between species and individual situation [69]. As expected, we observed
594 the smallest size of capsule in strains from HIV-infected patients, more likely reflecting
595 the fact that these strains might be more easily to cross biological barriers and to
596 disseminate in the brain in immunocompromised patients. However, the relationships
597 between capsule size and virulence have found controversial issues. One literature
598 reported that *C. neoformans* isolates with higher capsule formation were associated
599 with lower fungal clearance rates and increased intracranial pressure [70]. However,
600 this notion was disagreed by other groups, as their studies showed that *C. neoformans*
601 isolates with less capsule were more virulent and resulted in a higher fungal load in the
602 brain [54]. In order to verify that *in vitro* capsule and melanin production does reflect
603 the degree of pathogenicity, we test more virulence-related traits, including the ability
604 of *C. neoformans* to survive in human CSF, the level of macrophage uptake, and
605 morbidity in mouse model of cryptococcosis. These *in vitro*, *ex vivo* and *in vivo* data

606 sustain the importance of host environment on the virulence evolution of *C. neoformans*.
607 Actually, our findings are well consistent with the study by Robertson *et al.* [70].
608 Considering an impaired immune system in the HIV-infected patients, it is reasonable
609 to conclude that virulence may not be an important factor in establishment of a
610 successful infection. However, for colonization in a relatively healthy individual, such
611 as HIV-negative patients, the cryptococcal strains must evolve to enhance their traits in
612 virulence, in order to fight against the host immune system.

613 Mutation represents the ultimate source of the genetic variation required for adaptation
614 and most of time the genomic mutation rate is adjusted to a level that best promote
615 adaptation. We hypothesized that changes due to highly frequent genetic variations may
616 contribute to the observed virulence variabilities among strains derived from different
617 groups. To our surprise, we found that it is not the case, the basis of virulence
618 attenuation and the multiple phenotypic changes of strains from HIV-infected group
619 was unable to be largely addressed by the genomic changes at a high frequency.
620 Consistently, a previous whole-genome sequencing study in 32 isolates from 18 South
621 African patients with recurrent cryptococcal meningitis also revealed that only a few
622 genetic changes, including single nucleotide polymorphism (SNPs), small
623 insertions/deletions (indels) and variation in copy number, were identified between
624 incident and relapse isolates [71]. However, we did observe genetic variations for a
625 few specific genes in these two groups. For example, the isolates from HIV-uninfected
626 group harbor frequent genomic mutations identified in a list of genes specifically
627 related to environmental adaptation, which could explain the increased virulent
628 phenotypes of this group when compared to the strains from HIV-infected group.
629 Genetic mutations actively respond to the change of host environment and thereby drive

630 the adaptive evolution of fungal virulence. In contrast, we observed in HIV-infected
631 group that genetic variations were mostly occurred in genes associated with metabolic
632 processes, implying that the mutations may significantly correlate with survival with
633 respect to the possible role of these genes in receiving nutrients from the host, which is
634 expected to have almost no immune stresses.

635 In conclusion, through successful combination of genotyping, pathogenic phenotyping
636 and comparative genomics, our work has for the first time performed phenotypic
637 characterization and evaluated virulence-related properties of *C. neoformans* strains
638 isolated from three different host environments, including the HIV-uninfected
639 individuals, HIV-infected patients and the natural resources. Our studies highlighted
640 that host environmental factors may majorly account for the attenuation of virulence
641 and various other phenotypic changes in the strains from HIV-infected patients that are
642 different from their HIV-uninfected counterparts. Moreover, our work also supports an
643 essential role of the genetic variations in driving the evolution of fungal virulence. This
644 might be extremely important for *C. neoformans* to avoid clearance of host immunity
645 and establish successful colonization. Further biochemical, molecular genetics and
646 immunological studies are required to confirm and assess the relative importance of
647 both environmental and genetic factors in regulating pathogenicity and causing
648 invasive infection of *C. neoformans*. Such studies will not only improve our
649 understanding of pathogenic mechanisms of this fungus but also facilitate design of
650 new therapeutic approaches based on these factors.

651 **Acknowledgments**

652 The authors would like to convey gratitude to Prof. Liao Wanqing (Department of
653 Dermatology, Changzheng Hospital, Second Military University, Shanghai, China),
654 Prof. Xue Chaoyang (The Rutgers University, USA) for valuable comments, sharing
655 strains and providing human CSF samples. The authors also thank all members of the
656 Chen-lab for helpful advice and discussion. CC is supported by grants from the MOST
657 Key R&D Program (2020YFA0907200); National Natural Science Foundation of
658 China (31870141, 31570140); the Key Research Program of the Chinese Academy of
659 Sciences (KGFZD-135-19-11,153831KYSB20170043); the Innovation Capacity
660 Building Project of Jiangsu Province (BM2020019). JZ is supported by the National
661 Natural Science Foundation of China (81874240) and Natural Science Foundation of
662 Shanghai (16ZR1432400). HL is supported by the Special Program (19SWAQ18) and
663 Open Project of the State Key Laboratory of Trauma, Burns and Combined Injury
664 (SKLKF201803). XH is supported by the National Natural Science Foundation of
665 China to (32070146, 31600119); Youth Innovation Promotion Association, CAS;
666 Natural Science Foundation of Shanghai (20ZR1463800, 15ZR1444400). CC and JZ
667 conceived and designed the research study and wrote the paper; WY and YY performed
668 the experiments, analyzed the data and wrote the paper; LL and GL collected the strains
669 from HIV-infected patients and analyzed the data; XC, ML, TZ, HL, XH and TJ
670 analyzed the data. LZ and MC provided strains from HIV-uninfected patients and the
671 natural resources. All authors read and approved the final version of the paper.

672 **Conflict of interest**

673 The authors declare that they have no conflict of interest.

674 **References**

- 675 1. Kwon-Chung KJ, Varma A. Do major species concepts support one, two or more species within
676 *Cryptococcus neoformans*? FEMS Yeast Res. 2006;6(4):574-87. doi: 10.1111/j.1567-
677 1364.2006.00088.x. PubMed PMID: 16696653.
- 678 2. Cogliati M. Global Molecular Epidemiology of *Cryptococcus neoformans* and *Cryptococcus gattii*:
679 An Atlas of the Molecular Types. Scientifica (Cairo). 2013;2013:675213. doi: 10.1155/2013/675213.
680 PubMed PMID: 24278784; PubMed Central PMCID: PMC3820360.
- 681 3. Kidd SE, Hagen F, Tschärke RL, Huynh M, Bartlett KH, Fyfe M, et al. A rare genotype of
682 *Cryptococcus gattii* caused the cryptococcosis outbreak on Vancouver Island (British Columbia, Canada).
683 Proc Natl Acad Sci U S A. 2004;101(49):17258-63. doi: 10.1073/pnas.0402981101. PubMed PMID:
684 15572442; PubMed Central PMCID: PMC3535360.
- 685 4. Guo LY, Liu LL, Liu Y, Chen TM, Li SY, Yang YH, et al. Characteristics and outcomes of
686 cryptococcal meningitis in HIV seronegative children in Beijing, China, 2002-2013. BMC Infect Dis.
687 2016;16(1):635. doi: 10.1186/s12879-016-1964-6. PubMed PMID: 27814690; PubMed Central PMCID:
688 PMC35097362.
- 689 5. Chen M, Xu Y, Hong N, Yang Y, Lei W, Du L, et al. Epidemiology of fungal infections in China.
690 Front Med. 2018;12(1):58-75. doi: 10.1007/s11684-017-0601-0. PubMed PMID: 29380297.
- 691 6. Rajasingham R, Smith RM, Park BJ, Jarvis JN, Govender NP, Chiller TM, et al. Global burden of
692 disease of HIV-associated cryptococcal meningitis: an updated analysis. Lancet Infect Dis.
693 2017;17(8):873-81. doi: 10.1016/S1473-3099(17)30243-8. PubMed PMID: 28483415; PubMed Central
694 PMCID: PMC5818156.
- 695 7. Wu SY, Lei Y, Kang M, Xiao YL, Chen ZX. Molecular characterisation of clinical *Cryptococcus*
696 *neoformans* and *Cryptococcus gattii* isolates from Sichuan province, China. Mycoses. 2015;58(5):280-
697 7. doi: 10.1111/myc.12312. PubMed PMID: 25808662.
- 698 8. Alves GS, Freire AK, Bentes Ados S, Pinheiro JF, de Souza JV, Wanke B, et al. Molecular typing
699 of environmental *Cryptococcus neoformans*/C. *gattii* species complex isolates from Manaus, Amazonas,
700 Brazil. Mycoses. 2016;59(8):509-15. doi: 10.1111/myc.12499. PubMed PMID: 27005969.
- 701 9. Benham RW. Cryptococcosis and blastomycosis. Ann N Y Acad Sci. 1950;50(10):1299-314. doi:
702 10.1111/j.1749-6632.1950.tb39828.x. PubMed PMID: 14783320.
- 703 10. Evans EE. The antigenic composition of *Cryptococcus neoformans*. I. A serologic classification by
704 means of the capsular and agglutination reactions. J Immunol. 1950;64(5):423-30. PubMed PMID:
705 15415610.
- 706 11. Wilson DE, Bennett JE, Bailey JW. Serologic grouping of *Cryptococcus neoformans*. Proc Soc Exp
707 Biol Med. 1968;127(3):820-3. doi: 10.3181/00379727-127-32812. PubMed PMID: 5651140.
- 708 12. Kwon-Chung KJ, Boekhout T, Fell JW, Diaz M. (1557) Proposal to conserve the name
709 *Cryptococcus gattii* against *C. honduricus* and *C. bacillisporus* (Basidiomycota, Hymenozygomycetes,
710 Tremellomycetidae). Taxon. 2002;51(4):804-6.
- 711 13. Park BJ, Wannemuehler KA, Marston BJ, Govender N, Pappas PG, Chiller TM. Estimation of the
712 current global burden of cryptococcal meningitis among persons living with HIV/AIDS. Aids.
713 2009;23(4):525-30.
- 714 14. Dromer F, Mathoulin S, Dupont B, Letenneur L, Ronin O, Group FCS. Individual and
715 environmental factors associated with infection due to *Cryptococcus neoformans* serotype D. Clinical
716 infectious diseases. 1996;23(1):91-6.
- 717 15. Kwon-Chung KJ, Edman JC, Wickes BL. Genetic association of mating types and virulence in
718 *Cryptococcus neoformans*. Infection and immunity. 1992;60(2):602-5.

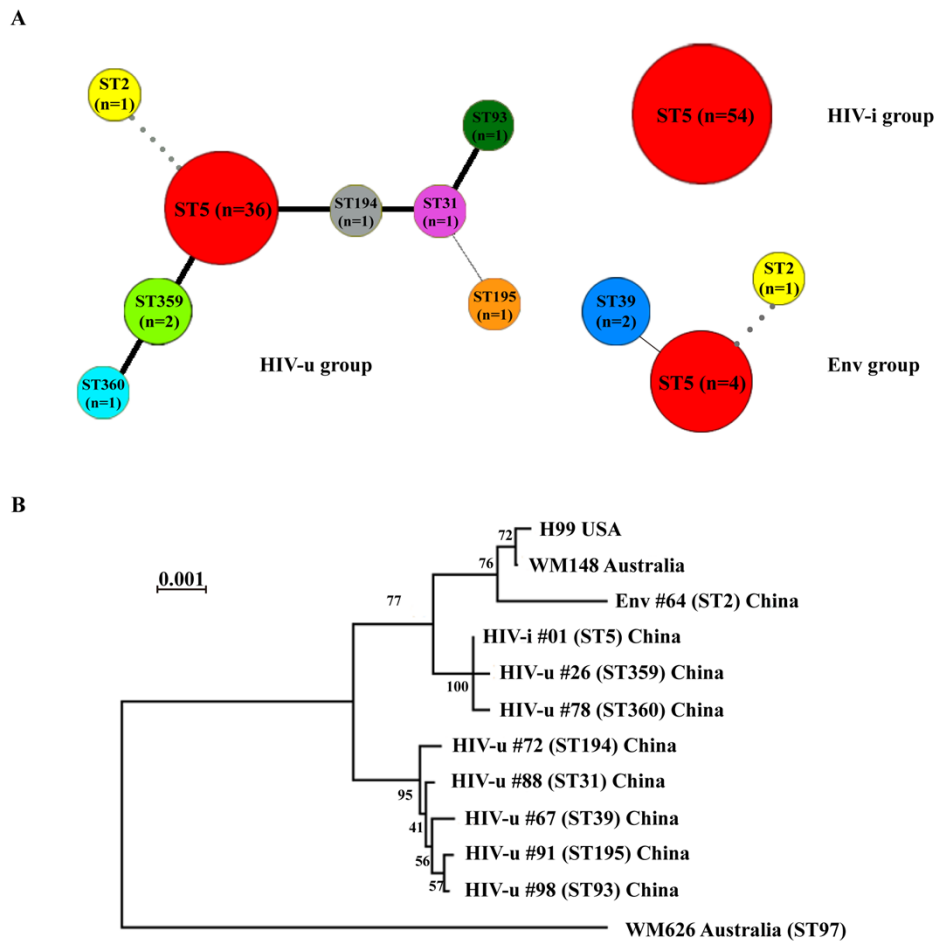
- 719 16. Meyer W, Castaneda A, Jackson S, Huynh M, Castaneda E, IberoAmerican Cryptococcal Study G.
720 Molecular typing of IberoAmerican Cryptococcus neoformans isolates. *Emerg Infect Dis*.
721 2003;9(2):189-95. doi: 10.3201/eid0902.020246. PubMed PMID: 12603989; PubMed Central PMCID:
722 PMCPMC2901947.
- 723 17. Boekhout T, Theelen B, Diaz M, Fell JW, Hop WCJ, Abeln ECA, et al. Hybrid genotypes in the
724 pathogenic yeast *Cryptococcus neoformans*. *Microbiology (Reading)*. 2001;147(Pt 4):891-907. doi:
725 10.1099/00221287-147-4-891. PubMed PMID: 11283285.
- 726 18. Meyer W, Aanensen DM, Boekhout T, Cogliati M, Diaz MR, Esposto MC, et al. Consensus multi-
727 locus sequence typing scheme for *Cryptococcus neoformans* and *Cryptococcus gattii*. *Med Mycol*.
728 2009;47(6):561-70. doi: 10.1080/13693780902953886. PubMed PMID: 19462334; PubMed Central
729 PMCID: PMCPMC2884100.
- 730 19. Cuomo CA, Rhodes J, Desjardins CA. Advances in *Cryptococcus* genomics: insights into the
731 evolution of pathogenesis. *Mem Inst Oswaldo Cruz*. 2018;113(7):e170473. doi: 10.1590/0074-
732 02760170473. PubMed PMID: 29513784; PubMed Central PMCID: PMCPMC5851040.
- 733 20. Hagen F, Colom MF, Swinne D, Tintelnot K, Iatta R, Montagna MT, et al. Autochthonous and
734 dormant *Cryptococcus gattii* infections in Europe. *Emerg Infect Dis*. 2012;18(10):1618-24. doi:
735 10.3201/eid1810.120068. PubMed PMID: 23017442; PubMed Central PMCID: PMCPMC3471617.
- 736 21. Antinori S. New Insights into HIV/AIDS-Associated Cryptococcosis. *ISRN AIDS*.
737 2013;2013:471363. doi: 10.1155/2013/471363. PubMed PMID: 24052889; PubMed Central PMCID:
738 PMCPMC3767198.
- 739 22. Litvintseva AP, Thakur R, Vilgalys R, Mitchell TG. Multilocus sequence typing reveals three
740 genetic subpopulations of *Cryptococcus neoformans* var. *grubii* (serotype A), including a unique
741 population in Botswana. *Genetics*. 2006;172(4):2223-38. doi: 10.1534/genetics.105.046672. PubMed
742 PMID: 16322524; PubMed Central PMCID: PMCPMC1456387.
- 743 23. Andrade-Silva LE, Ferreira-Paim K, Ferreira TB, Vilas-Boas A, Mora DJ, Manzato VM, et al.
744 Genotypic analysis of clinical and environmental *Cryptococcus neoformans* isolates from Brazil reveals
745 the presence of VNB isolates and a correlation with biological factors. *PLoS One*. 2018;13(3):e0193237.
746 doi: 10.1371/journal.pone.0193237. PubMed PMID: 29505557; PubMed Central PMCID:
747 PMCPMC5837091.
- 748 24. Viviani MA, Cogliati M, Esposto MC, Lemmer K, Tintelnot K, Colom Valiente MF, et al.
749 Molecular analysis of 311 *Cryptococcus neoformans* isolates from a 30-month ECMM survey of
750 cryptococcosis in Europe. *FEMS Yeast Res*. 2006;6(4):614-9. doi: 10.1111/j.1567-1364.2006.00081.x.
751 PubMed PMID: 16696657.
- 752 25. Altamirano S, Jackson KM, Nielsen K. The interplay of phenotype and genotype in *Cryptococcus*
753 *neoformans* disease. *Biosci Rep*. 2020;40(10). doi: 10.1042/BSR20190337. PubMed PMID: 33021310;
754 PubMed Central PMCID: PMCPMC7569153.
- 755 26. Perfect JR, Dismukes WE, Dromer F, Goldman DL, Graybill JR, Hamill RJ, et al. Clinical practice
756 guidelines for the management of cryptococcal disease: 2010 update by the infectious diseases society
757 of america. *Clin Infect Dis*. 2010;50(3):291-322. doi: 10.1086/649858. PubMed PMID: 20047480;
758 PubMed Central PMCID: PMCPMC5826644.
- 759 27. Wiesner DL, Moskalenko O, Corcoran JM, McDonald T, Rolfes MA, Meya DB, et al. Cryptococcal
760 genotype influences immunologic response and human clinical outcome after meningitis. *mBio*.
761 2012;3(5). doi: 10.1128/mBio.00196-12. PubMed PMID: 23015735; PubMed Central PMCID:
762 PMCPMC3448160.
- 763 28. Beale MA, Sabiiti W, Robertson EJ, Fuentes-Cabrejo KM, O'Hanlon SJ, Jarvis JN, et al. Genotypic
764 Diversity Is Associated with Clinical Outcome and Phenotype in Cryptococcal Meningitis across

- 765 Southern Africa. *PLoS Negl Trop Dis*. 2015;9(6):e0003847. doi: 10.1371/journal.pntd.0003847.
766 PubMed PMID: 26110902; PubMed Central PMCID: PMCPMC4482434.
- 767 29. Chen J, Varma A, Diaz MR, Litvintseva AP, Wollenberg KK, Kwon-Chung KJ. *Cryptococcus*
768 *neoformans* strains and infection in apparently immunocompetent patients, China. *Emerg Infect Dis*.
769 2008;14(5):755-62. doi: 10.3201/eid1405.071312. PubMed PMID: 18439357; PubMed Central PMCID:
770 PMCPMC2600263.
- 771 30. Khayhan K, Hagen F, Pan W, Simwami S, Fisher MC, Wahyuningsih R, et al. Geographically
772 structured populations of *Cryptococcus neoformans* Variety *grubii* in Asia correlate with HIV status and
773 show a clonal population structure. *PLoS One*. 2013;8(9):e72222. doi: 10.1371/journal.pone.0072222.
774 PubMed PMID: 24019866; PubMed Central PMCID: PMCPMC3760895.
- 775 31. Day JN, Qihui S, Thanh LT, Trieu PH, Van AD, Thu NH, et al. Comparative genomics of
776 *Cryptococcus neoformans* var. *grubii* associated with meningitis in HIV infected and uninfected patients
777 in Vietnam. *PLoS Negl Trop Dis*. 2017;11(6):e0005628. doi: 10.1371/journal.pntd.0005628. PubMed
778 PMID: 28614360; PubMed Central PMCID: PMCPMC5484541.
- 779 32. Dou HT, Xu YC, Wang HZ, Li TS. Molecular epidemiology of *Cryptococcus neoformans* and
780 *Cryptococcus gattii* in China between 2007 and 2013 using multilocus sequence typing and the
781 *DiversiLab* system. *Eur J Clin Microbiol Infect Dis*. 2015;34(4):753-62. doi: 10.1007/s10096-014-2289-
782 2. PubMed PMID: 25471194.
- 783 33. Simwami SP, Khayhan K, Henk DA, Aanensen DM, Boekhout T, Hagen F, et al. Low diversity
784 *Cryptococcus neoformans* variety *grubii* multilocus sequence types from Thailand are consistent with an
785 ancestral African origin. *PLoS Pathog*. 2011;7(4):e1001343. doi: 10.1371/journal.ppat.1001343.
786 PubMed PMID: 21573144; PubMed Central PMCID: PMCPMC3089418.
- 787 34. Perfect JR. *Cryptococcus neoformans*: a sugar-coated killer with designer genes. *FEMS Immunol*
788 *Med Microbiol*. 2005;45(3):395-404. doi: 10.1016/j.femsim.2005.06.005. PubMed PMID: 16055314.
- 789 35. Beenhouwer DO, Shapiro S, Feldmesser M, Casadevall A, Scharff MD. Both Th1 and Th2
790 cytokines affect the ability of monoclonal antibodies to protect mice against *Cryptococcus neoformans*.
791 *Infect Immun*. 2001;69(10):6445-55. doi: 10.1128/IAI.69.10.6445-6455.2001. PubMed PMID:
792 11553589; PubMed Central PMCID: PMCPMC98780.
- 793 36. Kozel TR. Virulence factors of *Cryptococcus neoformans*. *Trends Microbiol*. 1995;3(8):295-9.
794 PubMed PMID: 8528612.
- 795 37. Zaragoza O. Basic principles of the virulence of *Cryptococcus*. *Virulence*. 2019;10(1):490-501. doi:
796 10.1080/21505594.2019.1614383. PubMed PMID: 31119976; PubMed Central PMCID:
797 PMCPMC6550552.
- 798 38. Mayer FL, Kronstad JW. Disarming Fungal Pathogens: *Bacillus safensis* Inhibits Virulence Factor
799 Production and Biofilm Formation by *Cryptococcus neoformans* and *Candida albicans*. *MBio*. 2017;8(5).
800 doi: 10.1128/mBio.01537-17. PubMed PMID: 28974618; PubMed Central PMCID: PMCPMC5626971.
- 801 39. Thompson JD, Higgins DG, Gibson TJ. CLUSTAL W: improving the sensitivity of progressive
802 multiple sequence alignment through sequence weighting, position-specific gap penalties and weight
803 matrix choice. *Nucleic Acids Res*. 1994;22(22):4673-80. PubMed PMID: 7984417; PubMed Central
804 PMCID: PMCPMC308517.
- 805 40. Liu OW, Chun CD, Chow ED, Chen C, Madhani HD, Noble SM. Systematic genetic analysis of
806 virulence in the human fungal pathogen *Cryptococcus neoformans*. *Cell*. 2008;135(1):174-88. doi:
807 10.1016/j.cell.2008.07.046. PubMed PMID: 18854164; PubMed Central PMCID: PMCPMC2628477.
- 808 41. García-Rodas R, Cordero RJ, Trevijano-Contador N, Janbon G, Moyrand F, Casadevall A, et al.
809 Capsule growth in *Cryptococcus neoformans* is coordinated with cell cycle progression. *MBio*.
810 2014;5(3):e00945-14.

- 811 42. Fernandes OdFL, Costa CR, Junior RdSL, Vinaud MC, e Souza LKH, de Paula JAM, et al. Effects
812 of *Pimenta pseudocaryophyllus* (Gomes) LR Landrum, on melanized and non-melanized *Cryptococcus*
813 *neoformans*. *Mycopathologia*. 2012;174(5-6):421-8.
- 814 43. Shulman JJ, Hontz A, Sedlis A, Walters AT, Balin H, LoSCUITO L. The Pap smear: take two.
815 *American journal of obstetrics and gynecology*. 1975;121(8):1024-8.
- 816 44. Hansakon A, Mutthakalin P, Ngamskulrungrroj P, Chayakulkeeree M, Angkasekwinai P.
817 *Cryptococcus neoformans* and *Cryptococcus gattii* clinical isolates from Thailand display diverse
818 phenotypic interactions with macrophages. *Virulence*. 2019;10(1):26-36.
- 819 45. Sabiiti W, Robertson E, Beale MA, Johnston SA, Brouwer AE, Loyse A, et al. Efficient
820 phagocytosis and laccase activity affect the outcome of HIV-associated cryptococcosis. *The Journal of*
821 *clinical investigation*. 2014;124(5):2000-8.
- 822 46. Denham ST, Verma S, Reynolds RC, Worne CL, Daugherty JM, Lane TE, et al. Regulated release
823 of cryptococcal polysaccharide drives virulence and suppresses immune infiltration into the central
824 nervous system. *Infect Immun*. 2017. doi: 10.1128/IAI.00662-17. PubMed PMID: 29203547; PubMed
825 Central PMCID: PMC5820953.
- 826 47. Guess T, Lai H, Smith SE, Sircy L, Cunningham K, Nelson DE, et al. Size Matters: Measurement
827 of Capsule Diameter in *Cryptococcus neoformans*. *J Vis Exp*. 2018;(132). doi: 10.3791/57171. PubMed
828 PMID: 29553511.
- 829 48. Tugume L, Rhein J, Hullsiek KH, Mpoza E, Kiggundu R, Ssebambulidde K, et al. HIV-associated
830 cryptococcal meningitis occurring at relatively higher CD4 counts. *The Journal of infectious diseases*.
831 2019;219(6):877-83.
- 832 49. Tamura K, Stecher G, Peterson D, Filipski A, Kumar S. MEGA6: Molecular Evolutionary Genetics
833 Analysis version 6.0. *Mol Biol Evol*. 2013;30(12):2725-9. doi: 10.1093/molbev/mst197. PubMed PMID:
834 24132122; PubMed Central PMCID: PMC3840312.
- 835 50. Dou H, Wang H, Xie S, Chen X, Xu Z, Xu Y. Molecular characterization of *Cryptococcus*
836 *neoformans* isolated from the environment in Beijing, China. *Med Mycol*. 2017;55(7):737-47. doi:
837 10.1093/mmy/myx026. PubMed PMID: 28431114.
- 838 51. Hull CM, Heitman J. Genetics of *Cryptococcus neoformans*. *Annu Rev Genet*. 2002;36:557-615.
839 doi: 10.1146/annurev.genet.36.052402.152652. PubMed PMID: 12429703.
- 840 52. Wickes BL. The role of mating type and morphology in *Cryptococcus neoformans* pathogenesis.
841 *Int J Med Microbiol*. 2002;292(5-6):313-29. doi: 10.1078/1438-4221-00216. PubMed PMID: 12452279.
- 842 53. Nielsen K, Heitman J. Sex and virulence of human pathogenic fungi. *Adv Genet*. 2007;57:143-73.
843 doi: 10.1016/S0065-2660(06)57004-X. PubMed PMID: 17352904.
- 844 54. Pool A, Lowder L, Wu Y, Forrester K, Rumbaugh J. Neurovirulence of *Cryptococcus neoformans*
845 determined by time course of capsule accumulation and total volume of capsule in the brain. *J Neurovirol*.
846 2013;19(3):228-38. doi: 10.1007/s13365-013-0169-7. PubMed PMID: 23733307.
- 847 55. Eisenman HC, Chow SK, Tse KK, McClelland EE, Casadevall A. The effect of L-DOPA on
848 *Cryptococcus neoformans* growth and gene expression. *Virulence*. 2011;2(4):329-36. doi:
849 10.4161/viru.2.4.16136. PubMed PMID: 21705857; PubMed Central PMCID: PMC3173677.
- 850 56. Johnston SA, May RC. *Cryptococcus* interactions with macrophages: evasion and manipulation of
851 the phagosome by a fungal pathogen. *Cellular microbiology*. 2013;15(3):403-11.
- 852 57. Smith LM, Dixon EF, May RC. The fungal pathogen *Cryptococcus neoformans* manipulates
853 macrophage phagosome maturation. *Cellular microbiology*. 2015;17(5):702-13.
- 854 58. García-Rodas R, Zaragoza O. Catch me if you can: phagocytosis and killing avoidance by

- 855 *Cryptococcus neoformans*. *FEMS Immunology & Medical Microbiology*. 2012;64(2):147-61.
- 856 59. Casadevall A, Coelho C, Cordero RJ, Dragotakes Q, Jung E, Vij R, et al. The capsule of
857 *Cryptococcus neoformans*. *Virulence*. 2019;10(1):822-31.
- 858 60. Gish SR, Maier EJ, Haynes BC, Santiago-Tirado FH, Srikanta DL, Ma CZ, et al. Computational
859 Analysis Reveals a Key Regulator of Cryptococcal Virulence and Determinant of Host Response. *MBio*.
860 2016;7(2):e00313-16. doi: 10.1128/mBio.00313-16. PubMed PMID: 27094327; PubMed Central
861 PMCID: PMC4850258.
- 862 61. Wang ZA, Li LX, Doering TL. Unraveling synthesis of the cryptococcal cell wall and capsule.
863 *Glycobiology*. 2018;28(10):719-30. doi: 10.1093/glycob/cwy030. PubMed PMID: 29648596; PubMed
864 Central PMCID: PMC6142866.
- 865 62. Casadevall A, Pirofski LA. Host-pathogen interactions: redefining the basic concepts of virulence
866 and pathogenicity. *Infect Immun*. 1999;67(8):3703-13. doi: 10.1128/IAI.67.8.3703-3713.1999. PubMed
867 PMID: 10417127; PubMed Central PMCID: PMC96643.
- 868 63. Urban M, Pant R, Raghunath A, Irvine AG, Pedro H, Hammond-Kosack KE. The Pathogen-Host
869 Interactions database (PHI-base): additions and future developments. *Nucleic Acids Res*.
870 2015;43(Database issue):D645-55. doi: 10.1093/nar/gku1165. PubMed PMID: 25414340; PubMed
871 Central PMCID: PMC4383963.
- 872 64. Bahn YS, Kojima K, Cox GM, Heitman J. A unique fungal two-component system regulates stress
873 responses, drug sensitivity, sexual development, and virulence of *Cryptococcus neoformans*. *Mol Biol*
874 *Cell*. 2006;17(7):3122-35. doi: 10.1091/mbc.e06-02-0113. PubMed PMID: 16672377; PubMed Central
875 PMCID: PMC1483045.
- 876 65. Bahn YS, Kojima K, Cox GM, Heitman J. Specialization of the HOG pathway and its impact on
877 differentiation and virulence of *Cryptococcus neoformans*. *Mol Biol Cell*. 2005;16(5):2285-300. doi:
878 10.1091/mbc.e04-11-0987. PubMed PMID: 15728721; PubMed Central PMCID: PMC1087235.
- 879 66. Okagaki LH, Wang Y, Ballou ER, O'Meara TR, Bahn YS, Alspaugh JA, et al. Cryptococcal titan
880 cell formation is regulated by G-protein signaling in response to multiple stimuli. *Eukaryot Cell*.
881 2011;10(10):1306-16. doi: 10.1128/EC.05179-11. PubMed PMID: 21821718; PubMed Central PMCID:
882 PMC3187071.
- 883 67. Hu G, Caza M, Bakkeren E, Kretschmer M, Bairwa G, Reiner E, et al. A P4-ATPase subunit of the
884 *Cdc50* family plays a role in iron acquisition and virulence in *Cryptococcus neoformans*. *Cell Microbiol*.
885 2017;19(6). doi: 10.1111/cmi.12718. PubMed PMID: 28061020; PubMed Central PMCID:
886 PMC5429215.
- 887 68. Choi YH, Ngamskulrungrroj P, Varma A, Sionov E, Hwang SM, Carriconde F, et al. Prevalence of
888 the VN1c genotype of *Cryptococcus neoformans* in non-HIV-associated cryptococcosis in the Republic
889 of Korea. *FEMS Yeast Res*. 2010;10(6):769-78. doi: 10.1111/j.1567-1364.2010.00648.x. PubMed PMID:
890 20561059; PubMed Central PMCID: PMC2920376.
- 891 69. Fernandes KE, Brockway A, Haverkamp M, Cuomo CA, van Ogtrop F, Perfect JR, et al. Phenotypic
892 Variability Correlates with Clinical Outcome in *Cryptococcus* Isolates Obtained from Botswanan
893 HIV/AIDS Patients. *MBio*. 2018;9(5). doi: 10.1128/mBio.02016-18. PubMed PMID: 30352938;
894 PubMed Central PMCID: PMC6199498.
- 895 70. Robertson EJ, Najjuka G, Rolfes MA, Akampurira A, Jain N, Anantharanjit J, et al. *Cryptococcus*
896 *neoformans* ex vivo capsule size is associated with intracranial pressure and host immune response in
897 HIV-associated cryptococcal meningitis. *J Infect Dis*. 2014;209(1):74-82. doi: 10.1093/infdis/jit435.
898 PubMed PMID: 23945372; PubMed Central PMCID: PMC3864387.
- 899 71. Chen Y, Farrer RA, Giamberardino C, Sakthikumar S, Jones A, Yang T, et al. Microevolution of
900 Serial Clinical Isolates of *Cryptococcus neoformans* var. *grubii* and *C. gattii*. *mBio*. 2017;8(2). doi:

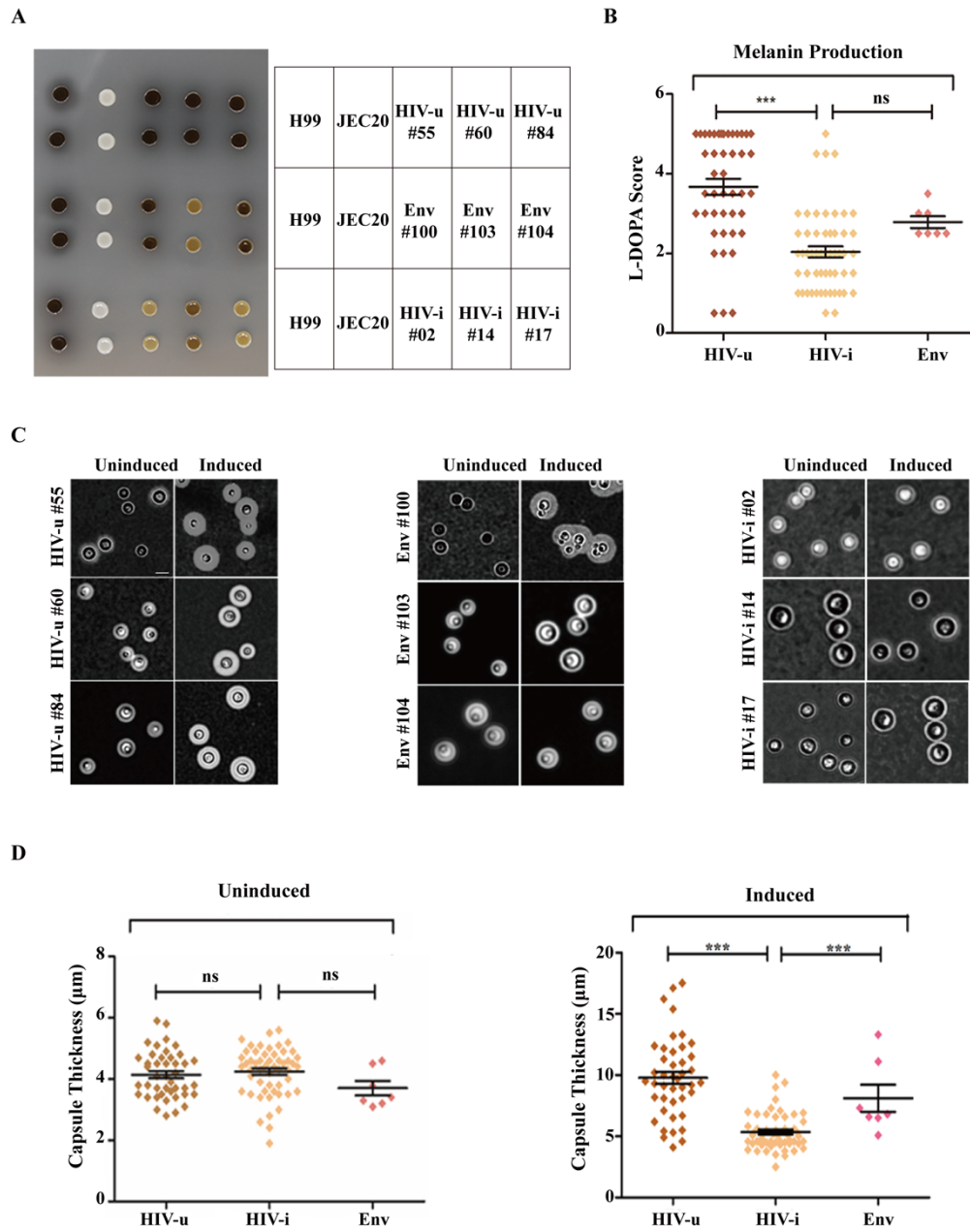
901 10.1128/mBio.00166-17. PubMed PMID: 28270580; PubMed Central PMCID: PMC5340869.



902

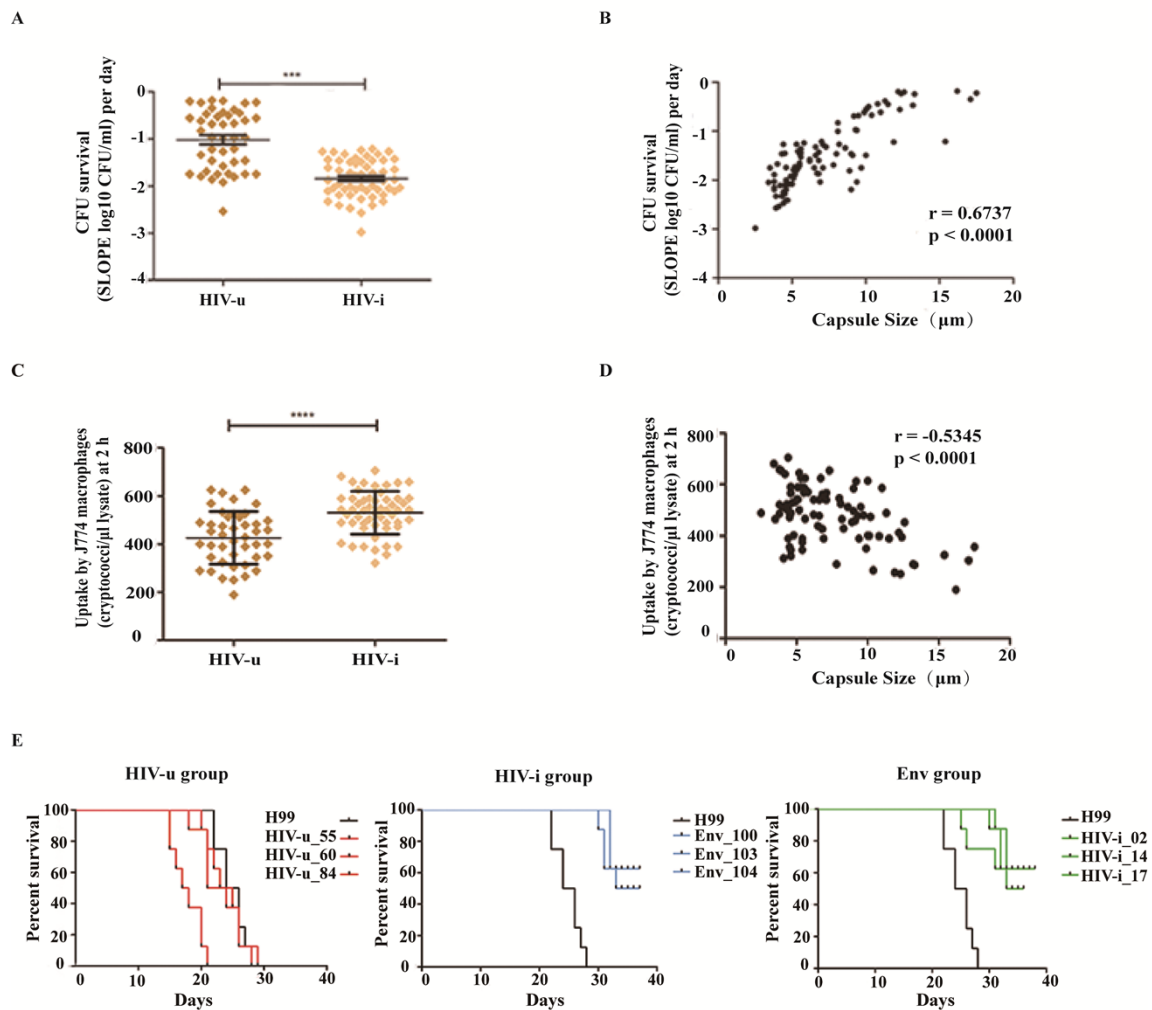
903 **Fig 1.** Genetic and evolutionary relationships among *C. neoformans* strains derived
 904 from different sources. **(A)** Hypothesis of the evolution of the 105 *C. neoformans*
 905 strains, based on phylogenetic relationships described by sequence analysis of the
 906 MLST scheme. Representative STs labelled with different colors. The number of
 907 isolates sharing the same ST is listed in each node, whereas the lines between STs
 908 indicate inferred phylogenetic relationships and are denoted by bold black, plain black,
 909 or grey line, depending on the number of allelic mismatches between profiles (bold
 910 black: < 3; Plain black: 3-4; Grey: > 4). **(B)** Phylogeny of selected *C. neoformans* strains

911 based on DNA sequences from eight housekeeping gene loci. The tree was constructed
 912 with the allelic frequencies using the neighbor-joining (NJ) model and 1,000 bootstrap
 913 replicates were performed. Numbers labeled with HIV-u, HIV-i or Env are strains from
 914 105 Chinese isolates in this study; Three reference strains, one from the United States
 915 and the other two from Australia, are also included.



916

917 **Fig 2.** *In vitro* characterization of melanin biosynthesis and the formation of
918 polysaccharide capsule in *Cryptococcus* isolates from each of the three groups. **(A)**
919 Three representative isolates were randomly selected from each group and melanin
920 phenotypes were verified by growth at 30 °C on plates containing L-DOPA. Pictures
921 were taken after incubation for 3 days. *C. neoformans* strains H99 and JEC20 were used
922 as positive and negative control, respectively. There were two replicates for each strain.
923 **(B)** Statistical comparison of melanin biosynthesis in all 105 isolates of *C. neoformans*.
924 The scores were calculated based on a K-Means cluster analysis. The vertical bars
925 represent standard errors of the means in each group. ns $p > 0.05$, *** $p < 0.001$. **(C)**
926 As in A, the same isolates were analyzed for capsule formation by India ink staining
927 under capsule-inducing and non-inducing growth conditions. A single colony from
928 each isolate was resuspended in PBS containing India ink, subjected to a short vortexing
929 and examined under a light microscope at $\times 63$ magnification. Scale bars, 10 μm . **(D)**
930 Statistical comparison of capsule formation in all 105 isolates of *C. neoformans*. As
931 described in Materials and Methods, stationary-phase fungal cultures were washed and
932 resuspended in PBS, and diluted 1/100 in capsule induction medium (10% Sabouraud
933 dextrose medium in MOPS buffered at pH 7.3). After incubation at 30 °C and 180rpm
934 for 48h, suspensions of India ink were photographed and the capsule thickness of each
935 isolate was measured. Each symbol represents the average capsule thickness of 10-20
936 cells. * $p < 0.05$, *** $p < 0.001$, by unpaired two-tailed Student's test.

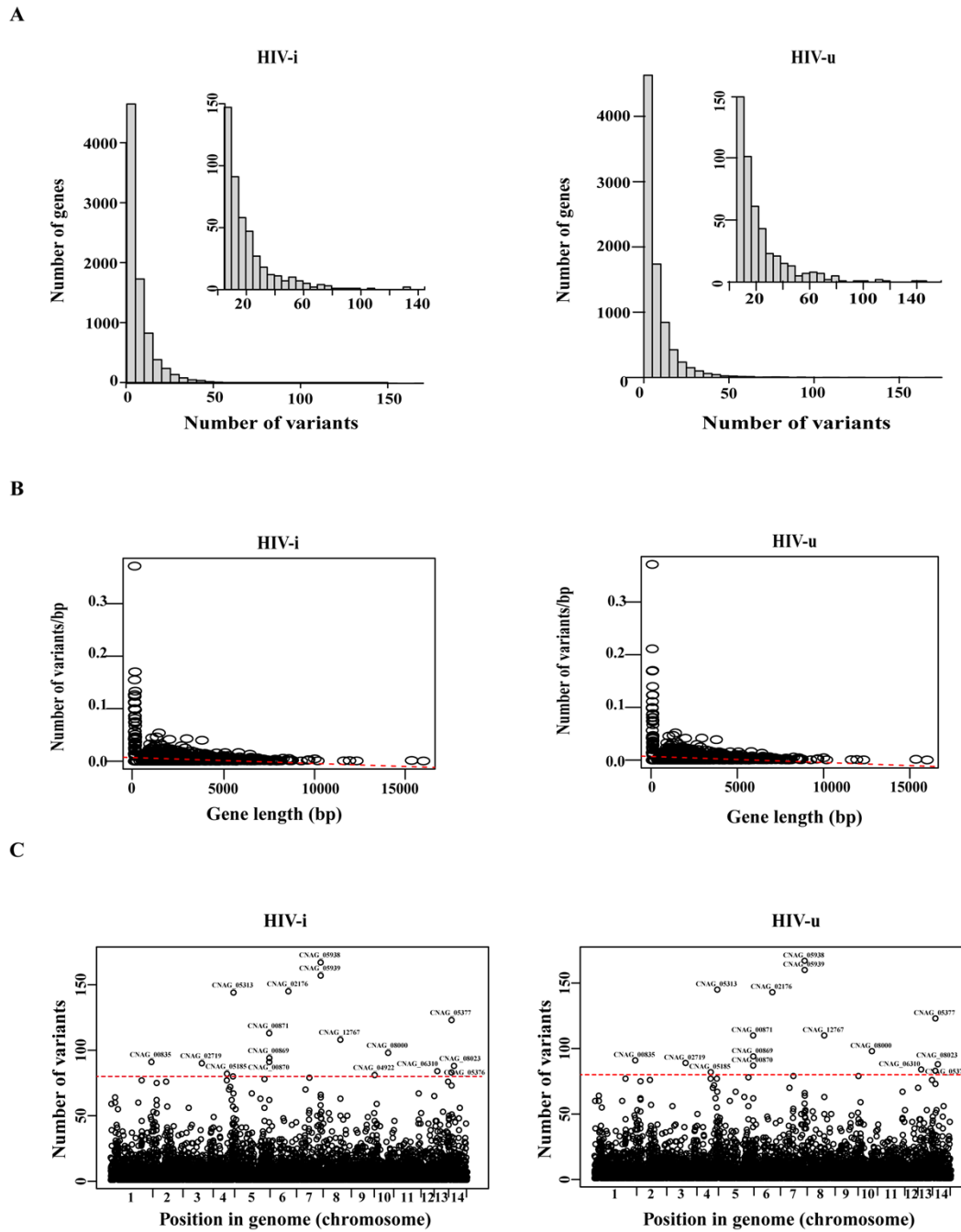


937

938

939 **Fig 3.** *Ex vivo* and *in vivo* assays investigating virulence-associated characteristics in
940 *Cryptococcus* isolates from each of the three groups. **(A, B)** Cryptococcal survival in
941 human CSF. Cells of each clinical isolate were inoculated into human CSF at a
942 concentration of $1\sim 2 \times 10^6$ cells/ml and aliquots were collected at different time points
943 (0,12, 24, 36,72 and 96 hours after inoculation) and plated on Sabouraud dextrose agar
944 (SDA) media for CFU counts. The survival slope was determined as the mean rate of
945 increase or decrease in cryptococcal counts after CSF treatment, by averaging the slope
946 of the linear regression of log₁₀ CFU/ml over time for each strain. A. Survival

947 comparison of clinical *C. neoformans* strains between HIV-u and HIV-i group after
948 incubation with human CSF; B. Association of capsule size with *ex vivo* cryptococcal
949 survival in human CSF. **(C, D)** Phagocytic uptake of clinical *C. neoformans* strains by
950 macrophage-like cell line J774. Macrophage cells (1.5×10^5) were incubated in serum-
951 free DMEM medium for 2 hours, activated with 15 μ g/ml phorbol myristate acetate
952 (PMA) for 30-60 minutes, and then co-incubated with *C. neoformans* yeast cells pre-
953 opsonized by a monoclonal antibody for 2 hours at 37°C with 5% CO₂ (MOI=1:10).
954 The extent of *Cryptococcus* phagocytosis was calculated as the number of cryptococci
955 internalized by macrophages 2 hours after infection. Results were expressed as the
956 mean of 3 to 4 experimental repeats. C. Phagocytic uptake comparison of clinical *C.*
957 *neoformans* strains between HIV-u and HIV-i group after incubation with J774; D.
958 Association of capsule size with *ex vivo* phagocytic uptake. **(E)** Kaplan-Meier survival
959 curves of mice infected with individual strains. Groups of female C57BL/6 mice (8 for
960 each group) were inoculated intranasally with 1×10^5 CFUs of the indicated strain and
961 monitored for progression to severe morbidity. As in Fig 2, the same three
962 representative isolates from each of the three groups were used. For comparison, the
963 strain H99 was used as a control. (Left) HIV-u group; (Middle) HIV-i group; and (Right)
964 Env group. Note: All *C. neoformans* strains, including the control strain H99 and all 9
965 tested isolates, were tested for pathogenicity in one experiment. *** $p < 0.001$, by Log-
966 rank test.



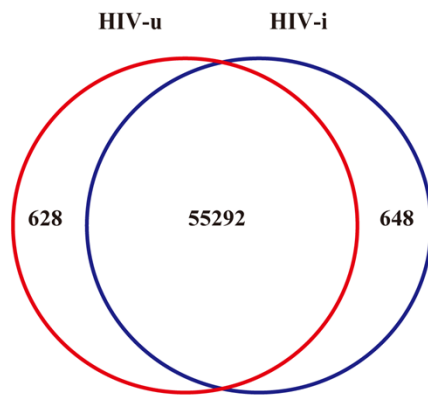
967

968 **Fig 4.** Summary of genomic variants identified from whole-genome sequencing of
 969 selected *C. neoformans* isolates. **(A)** A total of 28 clinical isolates, including 14 from
 970 the HIV-i group and another 14 from the HIV-u group, were sequenced. Shown is the
 971 number of variants that were identified in each gene locus. Genes with at least 20
 972 variants were selected and presented in the magnified inset panel. **(B)** All sequenced

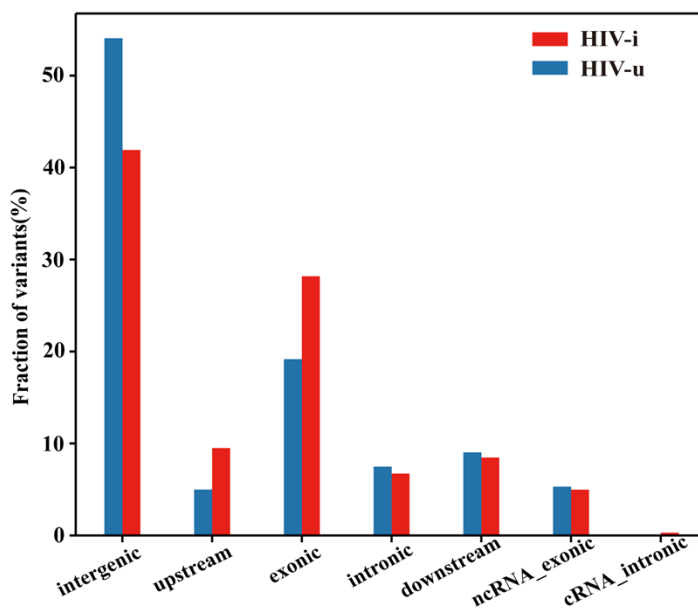
973 isolates from both groups showed no correlation between the number of variants and
974 gene length per base pair in each gene ($p < 0.5$). (C) Distribution of variants across the
975 genomes of sequenced isolates. Notably, a cluster of genes that were identical in both
976 groups had significantly high numbers of variants. Genes harboring more than 80
977 variants are indicated with their names.

978

A



B



979

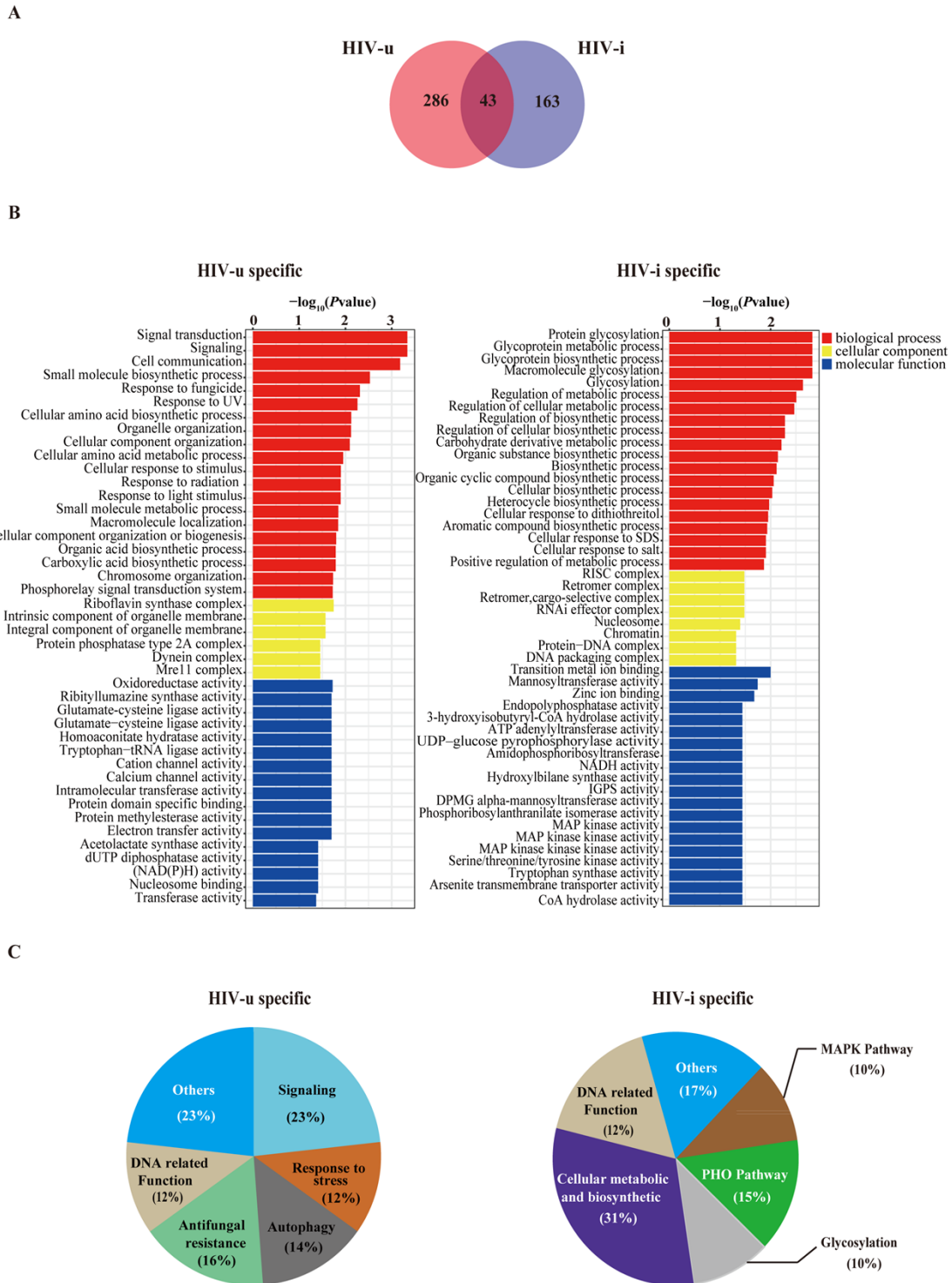
980

981 **Fig 5.** Common and group-specific variants identified in the sequenced isolates. **(A)**

982 Venn diagram showing a summary of the number of common or group-specific variants.

983 A common variant was defined as the one that are found in more than 7 isolates of each

984 group. **(B)** Genomic distribution of the group-specific variants.



985

986 **Fig 6.** Characterization of the genes harboring group-specific variants. **(A)** Venn

987 diagram showing the number of genes that were associated with group-specific variants.

988 It has to be noted that 43 genes are common in both groups only because the variants
 989 in each group were mapped to different positions of the same gene. **(B)** Significantly
 990 enriched Gene Ontology (GO) categories (p -value <0.05) with group-specific genes.
 991 **(C)** Functional classification pie chart showing the annotated genes that harbor group-
 992 specific variants, according to the Gene Ontology (GO) Term analysis

993 **Table 1.** Comparison of clinical data for HIV-uninfected and -infected groups

Parameter	Mean \pm SD (n) ^a			p -value ^c
	Total subjects ^b	Patients		
		HIV-u 44 isolates	HIV-i 51 isolates	
Age (yr)	41 \pm 11	38 \pm 9	43 \pm 12	0.0679
Sex (males/ females)	74/21	33/11	41/10	0.5792
CD4 Count (no. of cells/mm ³)	193 \pm 188	381 \pm 92	34 \pm 48	<0.001
Temperature ($^{\circ}$ C)	37.4 \pm 0.9	37.1 \pm 0.6	37.6 \pm 1.1	0.0037
Fever (Y/N)	45/50	12/32	33/18	<0.001
Headache(Y/N)	66/29	29/15	37/14	0.5105
Seizure(Y/N)	24/71	16/28	8/43	0.0207
Cerebral herniation(Y/N)	47/48	12/32	4/47	0.0143
Cerebellar Signs(Y/N)	16/79	28/16	20/31	0.0176

994 ^a Values, including age, CD4 counts and temperature, were represented by means \pm
 995 SD for the statistic characteristics and clinical parameters. *n* indicates the number of
 996 patients.

997 ^b Total subjects indicate the mean \pm SD of patients.

998 ^c *p* values were calculated by one-way ANOVA or Fisher's exact test as appropriate.

999 **Table 2.** Characterization of major genes harboring specific variations in HIV-u and
 1000 HIV-i groups, respectively

Function	Broad annotation	Gene name	Description	Classic fisher
Genes harboring specific variations in HIV-u group				
Response to stress	CNAG_03818	SSK1	Response to fungicide/UV/radiation/light stimulus	0.011
	CNAG_00769	PBS2	Cellular response to stimulus	0.013
Signaling	CNAG_05590	TCO2	Signaling, phosphorelay signal transduction system	0.001
	CNAG_06606	RHO104	Intracellular signal transduction	0.046
	CNAG_03751	Unknown	Cation(calcium) channel activity	0.022
	CNAG_02796	Unknown	Transferase activity, transferring alkyl or aryl groups	0.022
	CNAG_04599	Unknown	3-methyl-2-oxobutanoate hydroxymethy	0.022
	CNAG_05712	RIB4	Intramolecular transferase activity, transferring acyl groups	0.022
	CNAG_06806	ETF1alpha		

Antifungal resistance	CNAG_03582	RIM20	Macromolecule localization	0.023
	CNAG_05282	APT4		
	CNAG_05395	VAM6		
	CNAG_02565	Unknown	Organic acid biosynthetic process Carboxylic acid biosynthetic process	0.006
	CNAG_02796	Unknown		
	CNAG_05194	Unknown		
	CNAG_06421	Unknown		
	CNAG_04087	Unknown	Intrinsic and integral component of organelle membrane	0.032
	CNAG_04556	Unknown		
	CNAG_04604	Unknown	Tryptophan-tRNA ligase activity	0.022
CNAG_06421	Unknown	Ccetolactate synthase activity	0.044	
Autophagy	CNAG_02796	Unknown	Cellular amino acid metabolic and biosynthetic process	0.020
	CNAG_04599	Unknown		
	CNAG_06421	Unknown		
	CNAG_04484	Unknown	Organelle membrane fusion	0.022
Genes harboring specific variations in HIV-i group				
MAPK	CNAG_05063	SSK2	MAPK/ protein serine/threonine/tyrosine kinase activity	0.036
	CNAG_02853	Unknown	Amidophosphoribosyltransferase activity	0.036
PHO pathway	CNAG_04501	TRP1	Indole-3-glycerol-phosphate synthase activity, Phosphoribosylanthranilate isomerase activity	0.036
	CNAG_02506	RIB3	3,4-dihydroxy-2-butanone-4-phosphate synthase activity	0.0361
Glycosylation	CNAG_03832	KTR3	Glycoprotein metabolic and biosynthetic	0.011

			process, macromolecule glycosylation	
Cellular metabolism and biosynthesis	CNAG_00405	KIC1	Regulation of cellular and biosynthetic metabolic process	0.128
	CNAG_00745	HRK1	Regulation of biosynthetic process	0.015
	CNAG_01938	KIN1	Biosynthetic process	0.015
	CNAG_02090	GPA3	Carbohydrate derivative metabolic process	0.012
	CNAG_02305	FZC45	Organic substance biosynthetic process	0.006
	CNAG_06490	SNF102	Organic cyclic compound biosynthetic process	0.007
	CNAG_00678	URE7	Regulation of biological process	0.010
	CNAG_07679	DST1	Positive regulation of metabolic process	0.015
	CNAG_04755	BCK1	Aromatic compound biosynthetic process	0.019

1001